AVHRR Calibration (mostly)

Jerry Sullivan NOAA/NESDIS

presented at WWBG Mar. 13, 2007

1. AVHRR Thermal channel Calibraton
2. AVHRR Visible channel Calibration
3. SNOs (Simultaneous Nadir Overpass)
4. SNO applied to MSU (Microwave Sounding Unit)
5. Navigation

AVHRR Thermal channels

3B, 4, and 5

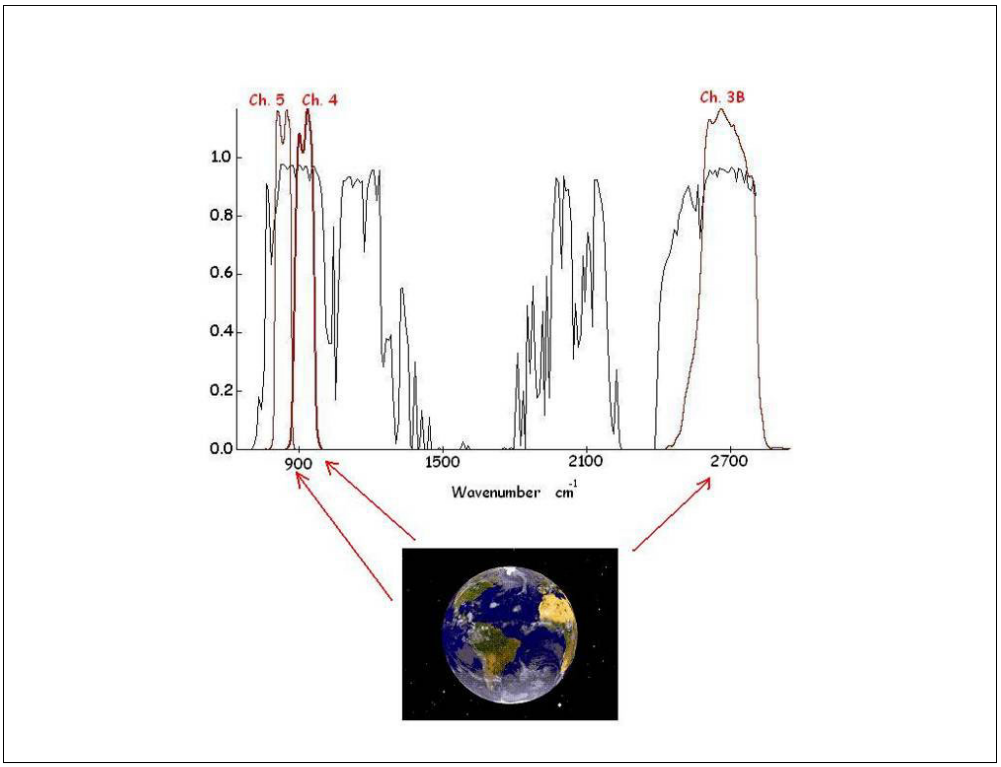

AVHRR thermal channel 3B, 4, and 5. They are “window” channels that mostly respond to surface or cloud radiation, and are slightly affected by water vapor (ch. 5 the most and ch. 3B the least). Chs. 4 and 5 respond solely to thermal radiation from the Earth, while ch. 3B also has a reflected solar component.

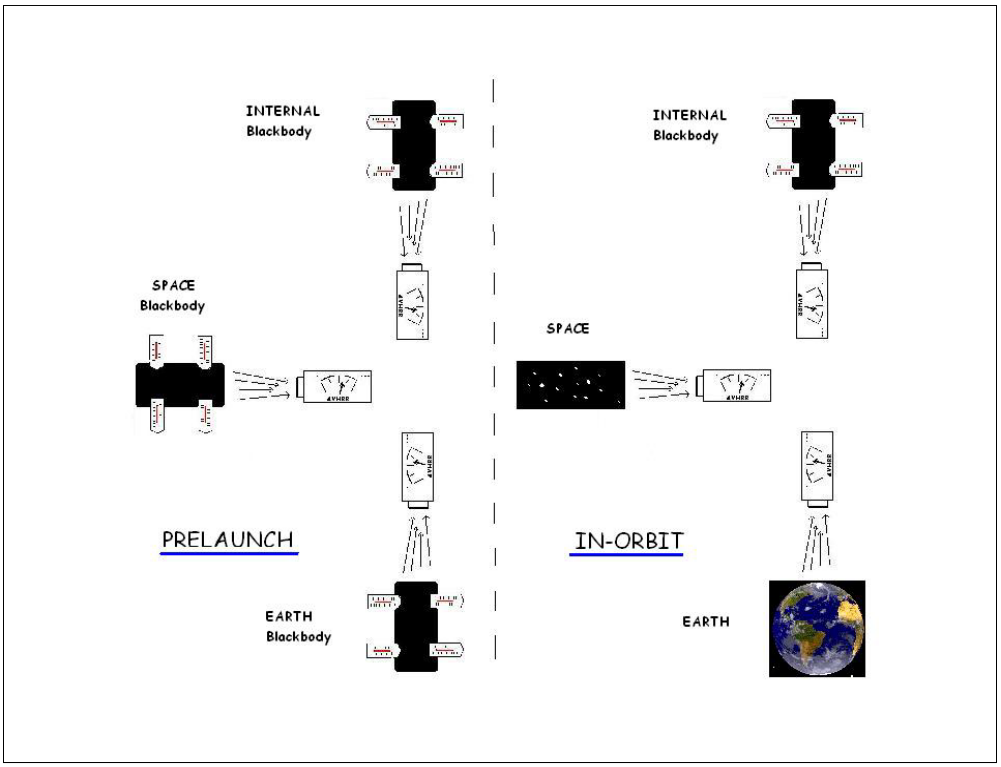

Prelaunch and In-orbit calibration sequences. Space is sampled first, 10 samples/counts. 2,048 Earth locations are then viewed. Finally, the internal blackbody target provides 10 samples. The internal blackbody is the same both in prelaunch and in-orbit.

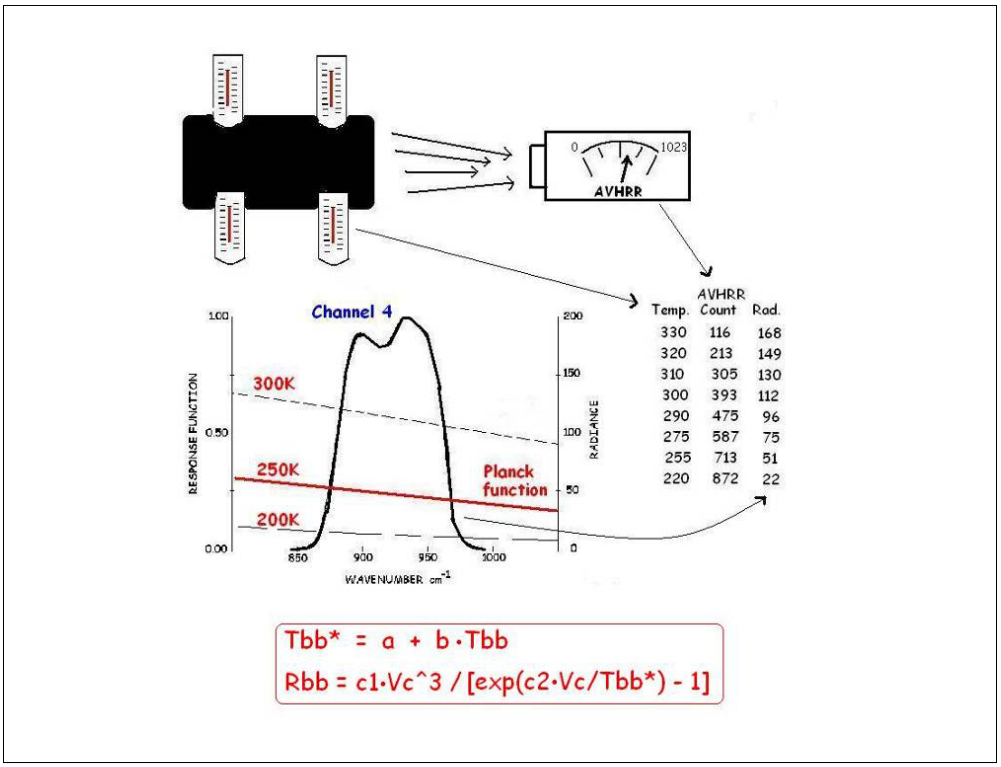

The basic calibration sequence: the AVHRR views a “constant-temperature” blackbody for 1 minute, and (hopefully) generates a constant AVHRR output count. This basic action is repeated for blackbody temperatures of 180, 220, 240, 255, 265, 275, … 335K, generating 17 (temperature, count) data points. The AVHRR responds to radiant energy, so an AVHRR radiance R at temperature T is generated by weighting the Planck function at wavenumber v by the AVHRR channel spectral response function SRF(v), giving 17 (radiance, count) data points. The T to R conversion is computed much more easily by the 2-step equation shown in red; accuracy usually better than 0.001K.

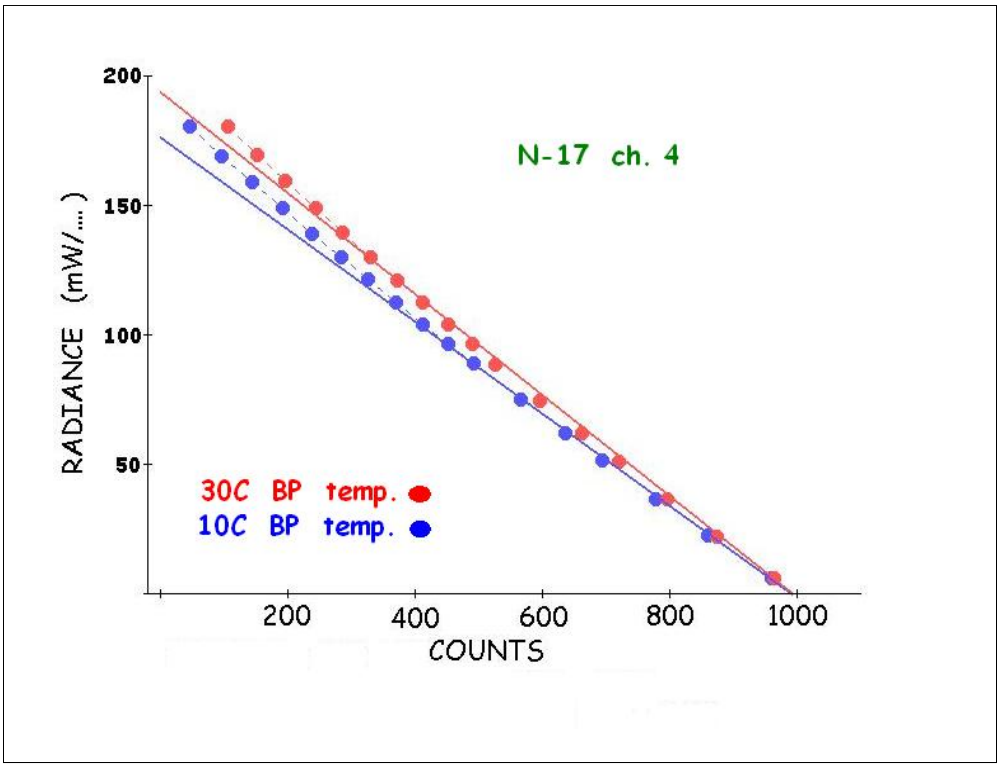

Nonlinear radiance correction #1. The solid red and blue lines are linear; the red and blue filled circles are measured radiances at different AVHRR instrument temperatures. The radiance vs. count curve is nonlinear, and the difference between the curve and the straight line varies with the instrument temperature.

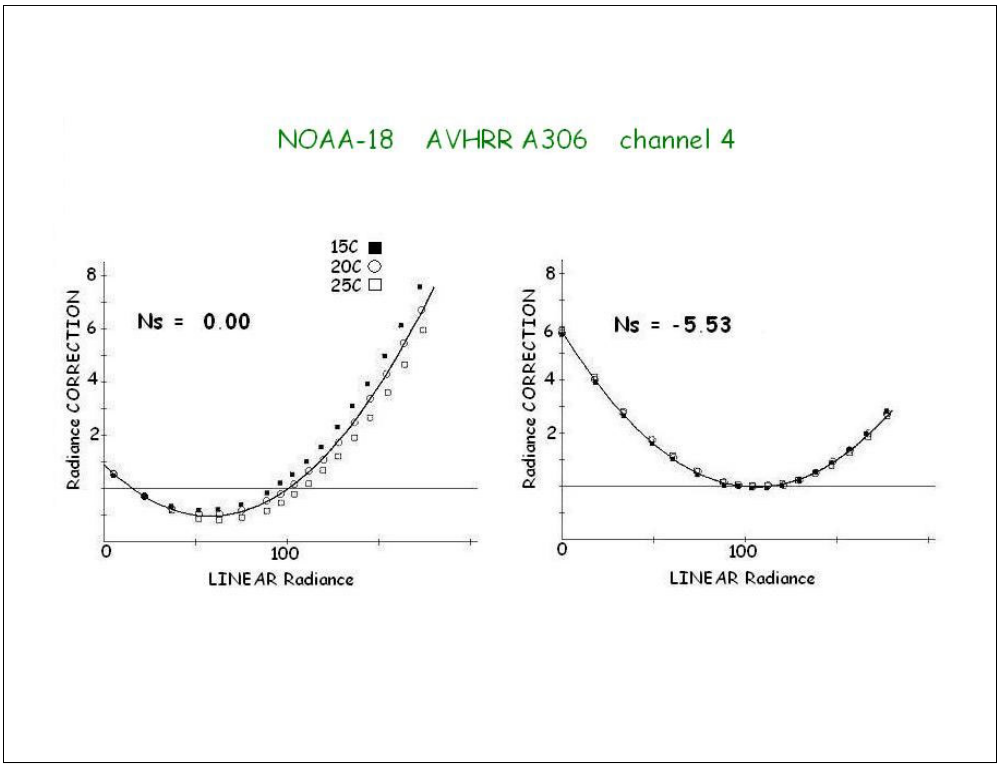

Nonlinear radiance correction #2. The left image shows the difference between the prelaunch measured data and a straight fit between the internal blackbody point (Cbb,Rbb) and the space point (Cs,Rs=0) for 3 different AVHRR operating temperatures. The correction curves depend on the instrument temperature. The right side shows correction curves when Rs= 0 is replaced by a (constant) non-zero Rs value; the 3 curves are almost identical.

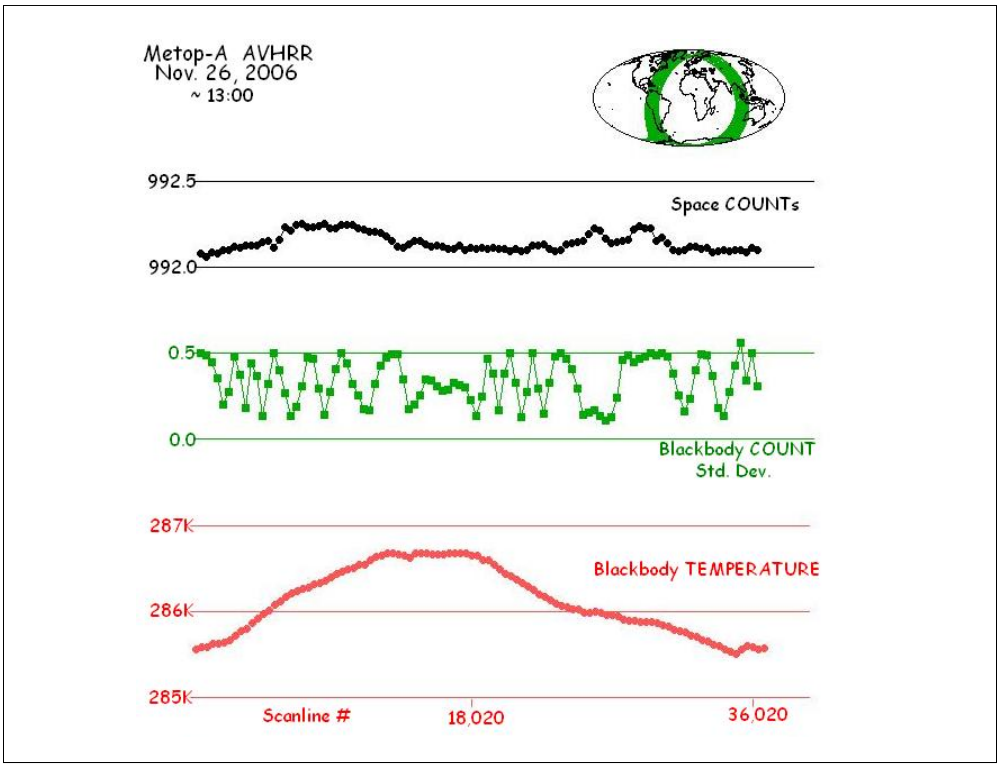

“Fingerprint” of the AVHRR in orbit !! The bottom curve plots 1-minute averages of the internal blackbody temperature as the AVHRR moves through a complete orbit. It varies by about 1K. The top graph shows 1-minute space count averages; the space count is clamped to about 992 counts. The middle curve plots moving 1-minute RMS values for blackbody counts around the 1-minute average count. In one minute, the blackbody temperature changes by only 0.01 – 0.02K, so the count value should be steady (RMS = 0.5 counts).

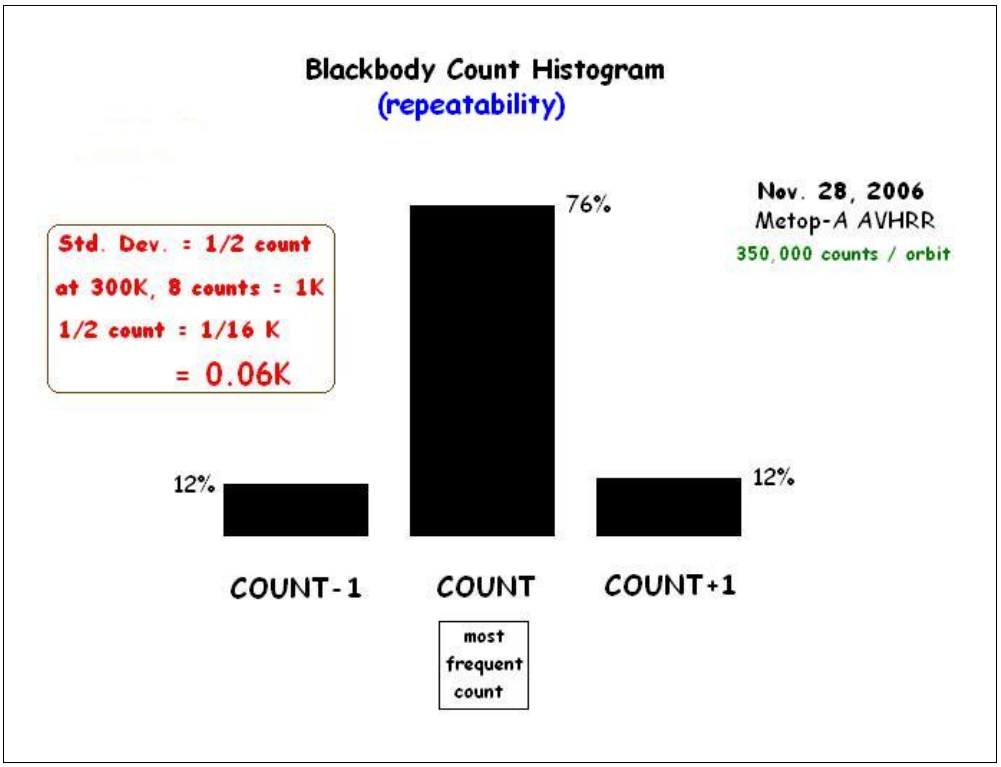

In a 1-minute interval, the BLACKBODY temperature typically varies by 0.01 – 0.02K; we can consider this a "constant" temperature. Because the source is constant, in this same 1-minute interval the AVHRR should output the same count value. In 99.9% of the 1-minute intervals I checked, around 75% of the counts had the same value COUNT (~ 475) and the remaining 25% had values within ± 1 count of COUNT. The standard deviation was ~ 0.5 counts. In the 300K region, a change of 0.5 counts = a change of 0.06K. So, when looking at a constant source, the AVHRR "thermal noise" is 0.06K which is twice as good as the specification of 0.12K.

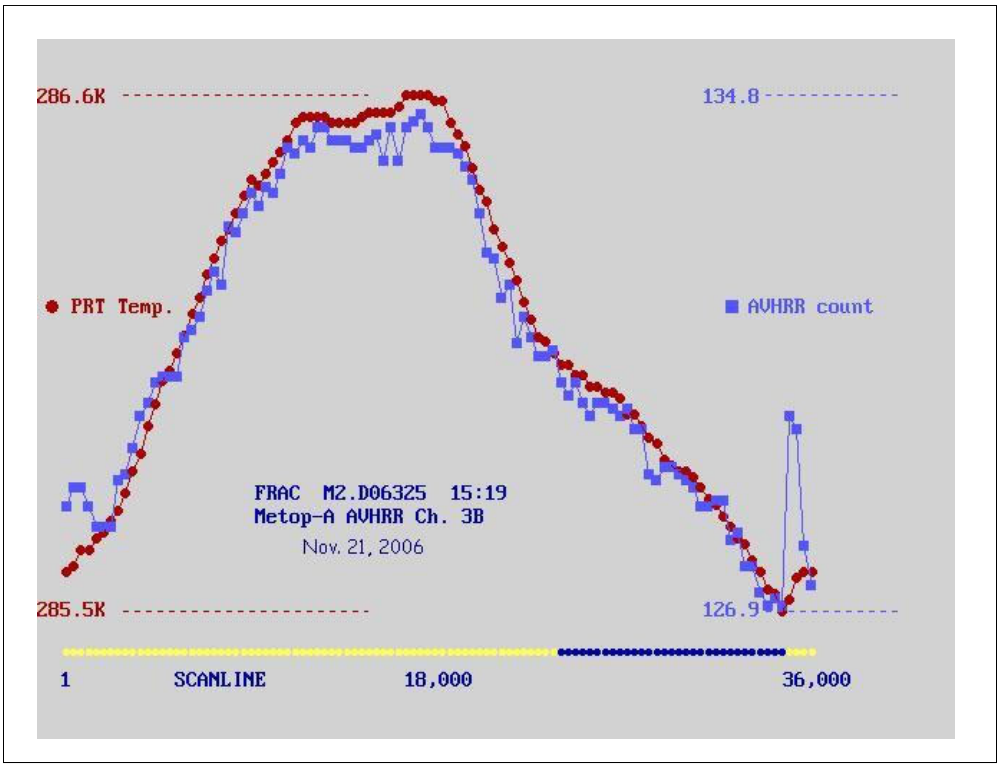

Stray light. In orbit, the Metop-A A305 AVHRR blackbody temperature varies by ~ 1K. In this small region, radiance is nearly linear with temperature, and count is nearly linear with radiance, so the count and temperature variations should be proportional. When both curves are scaled between min and MAX, and plotted against scanline, they lay nearly on top of each other. However, near the orbit end around scanline 36,000, there is an anomalous jump in AVHRR count output. This happens when the satellite is coming out of the dark (bottom line, yellow = sun, blue = darkness). Some stray (unwanted) energy affects the AVHRR. We see this in our morning satellites (the Metop-A overpass time = 9:30 in the morning), so the effect is expected.

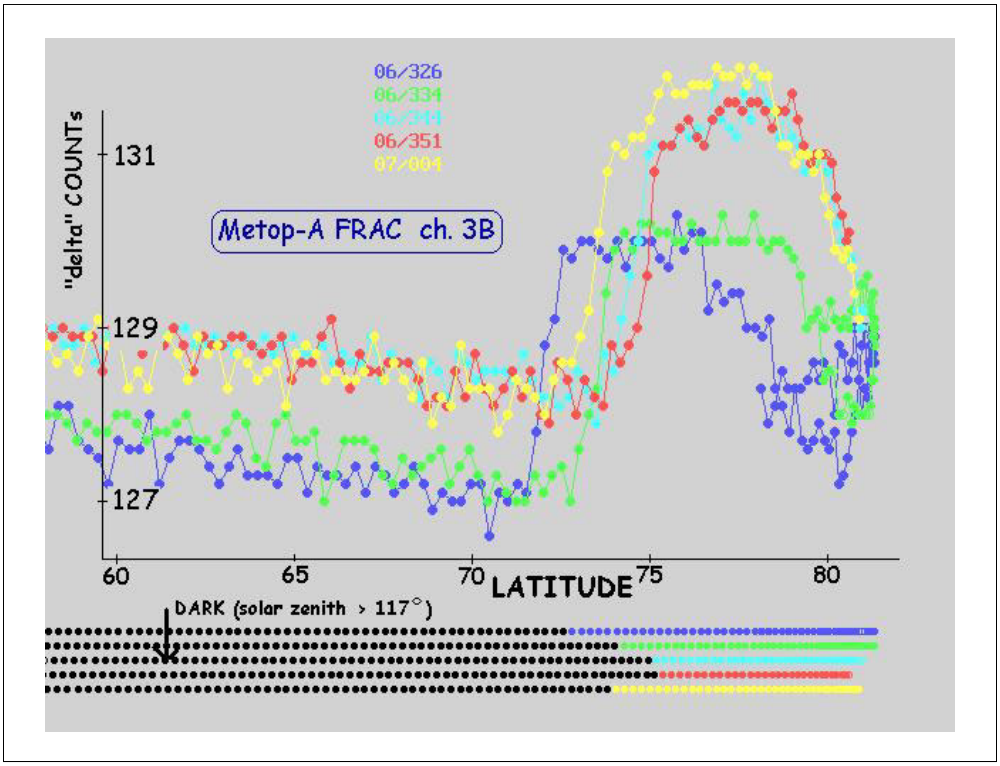

Stray light. The effect is seasonal. In late 2006, it occurred consistently around 72-73N latitude.

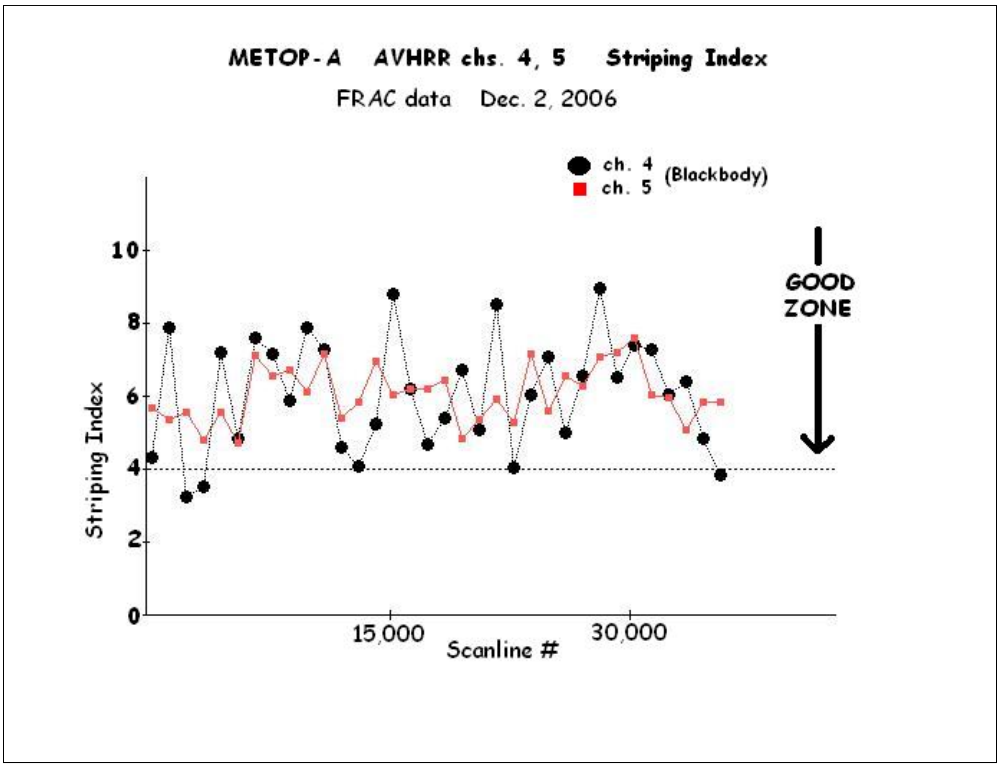

Striping Index. In a 1-minute sample of either space counts or blackbody counts (3,600 counts), the counts should be relatively constant. There is noise, usually + or – 1 count, but it should be random. In prelaunch for the original KLM AVHRR on the NOAA-15, the noise was not random. In some scanlines, all 10 counts were higher than the average, and in others all 10 counts were lower. This led to a striped appearance in simulated SST images, a sensitive temperature product. So, we now routinely check for striping using the ratio [within-line (random) variance]/[line-to-line variance] . Large values indicate small striping, and the Metop-A AVHRR A305 passed the test.

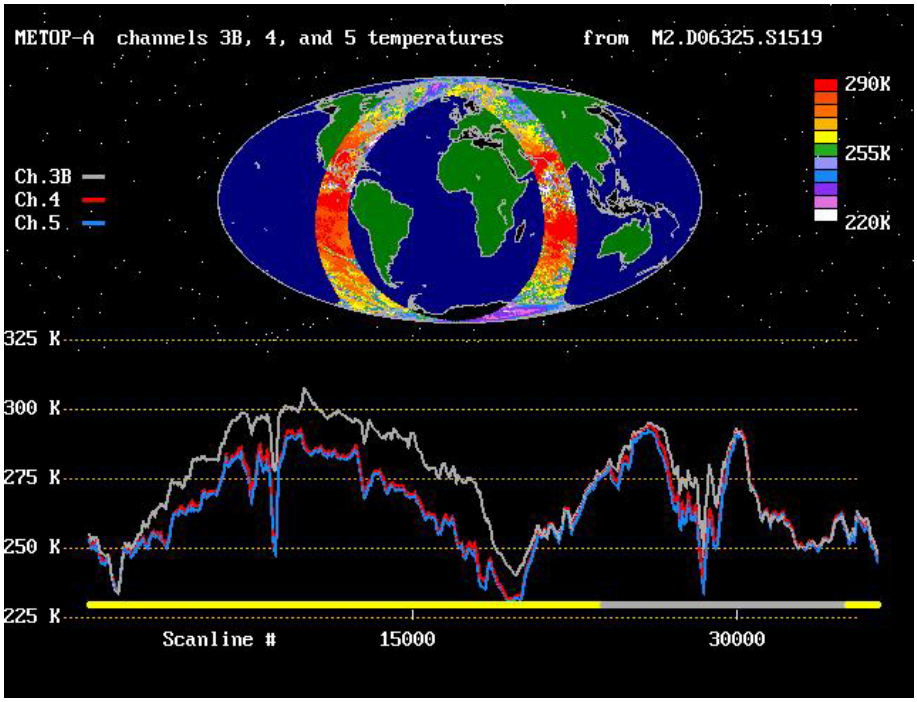

Nov. 21, 2006; the Metop-A A305 AVHRR thermal IR channels are on !! This ”Sanity Check” image makes sense. Desert temperatures approach 300K, consistent with a 9:30 morning orbit. Antarctic temperatures are near 225K, reasonable for the “warm” Antarctic summer. The sharp, downward spikes in the time series are from clouds in the ITCZ. When the horizontal line near the bottom is colored yellow, the satellite is in the sun. Channel 3B temperatures are noticeably warmer than channel 4 and 5 during this part of the orbit, because of the reflected solar radiation in channel 3B.

AVHRR Visible channels

1, 2, and 3A

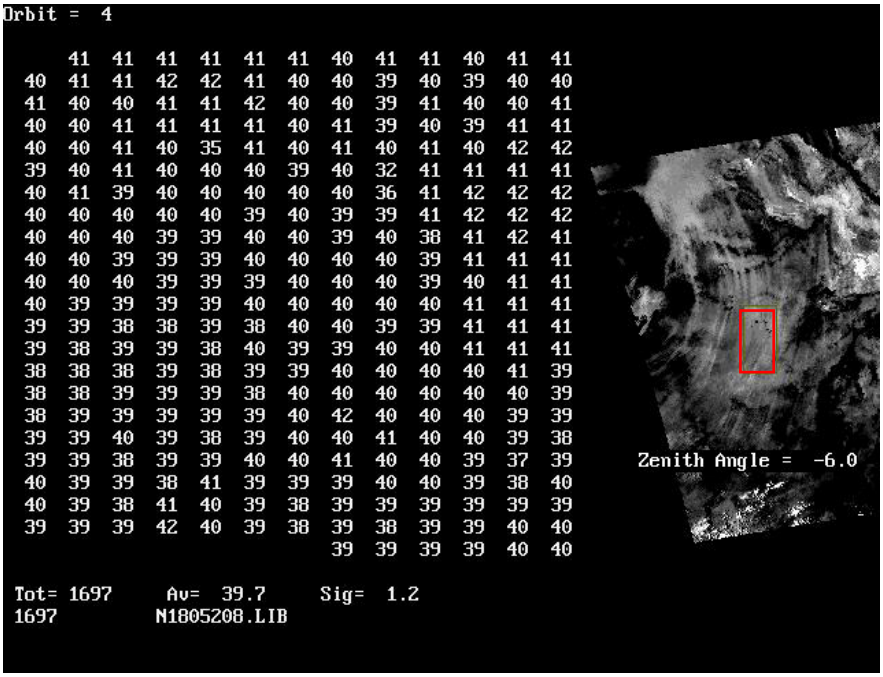

The Libyan Desert calibration target for AVHRR channels 1, 2, and 3A. It's large (~ New Hampshire), fairly homogeneous, and hopefully unchanging in time.

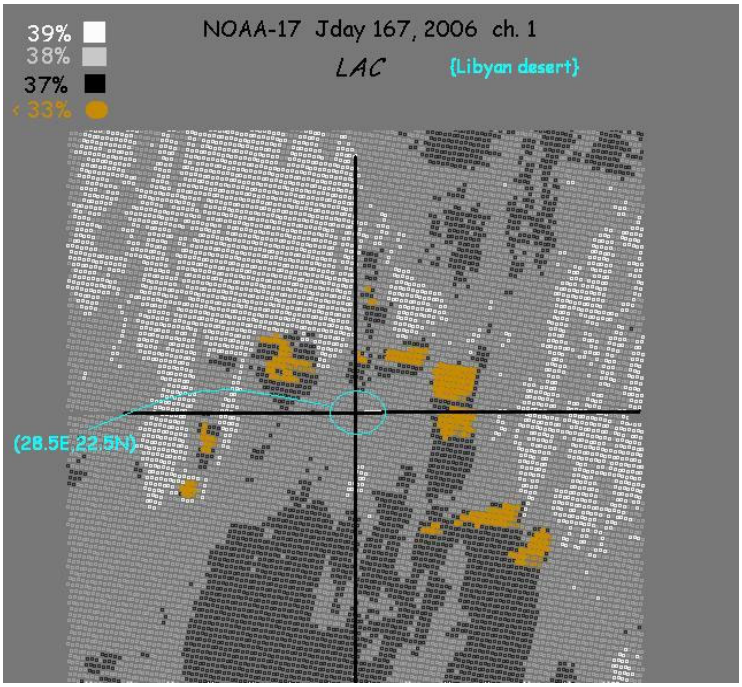

Note about “homogeneous” target; thanks to 1-km FRAC data and high-resolution Google Earth data. The areas in orange color are actually circular “somethings” , which look like circular pivot irrigation devices. They occupy only 1% of the target area and change the average reflectance by 0.1%, well below the noise level, so they cause no practical harm but are shocking.

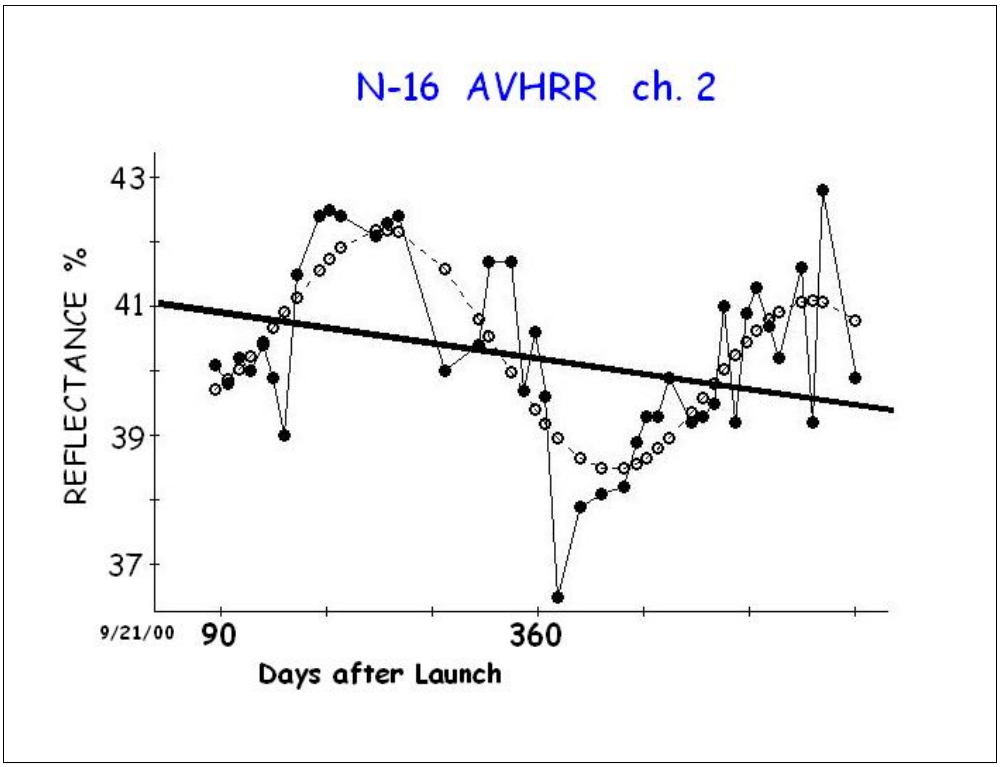

The effects of changing solar zenith and changing Earth-sun distance are accounted for in the VISIBLE channel calibration process. This seasonal effect, caused by the BDRF, is also taken into account.

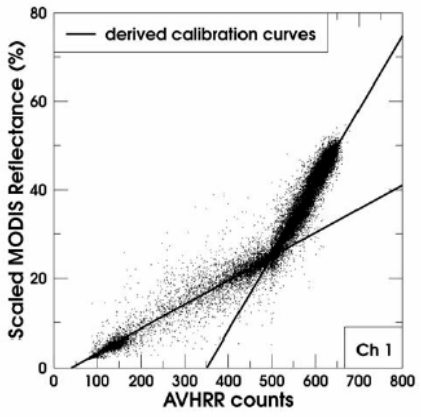

Figure 7. Variation of MODIS-derived AVHRR Ch1 reflectances with AVHRR Ch 1 counts.

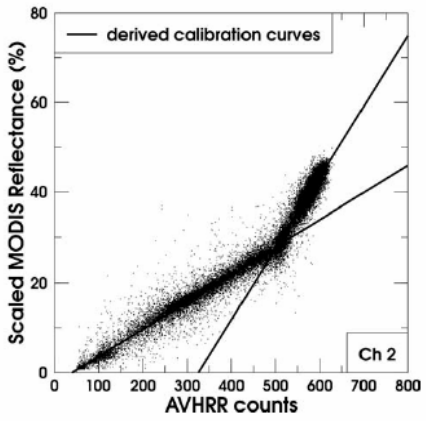

Figure 8. Variation of MODIS-derived AVHRR Ch2 reflectances with AVHRR Ch 2 counts.

Another VISIBLE channel calibration “headache”. Since the new AVHRR/3 model was introduced on the NOAA-15 AVHRR, the visible radiance vs. count straight line is now two, connected, straight lines. This was done to give more count range (more resolution) to reflectances in the 0-25% range, for the aerosol product.

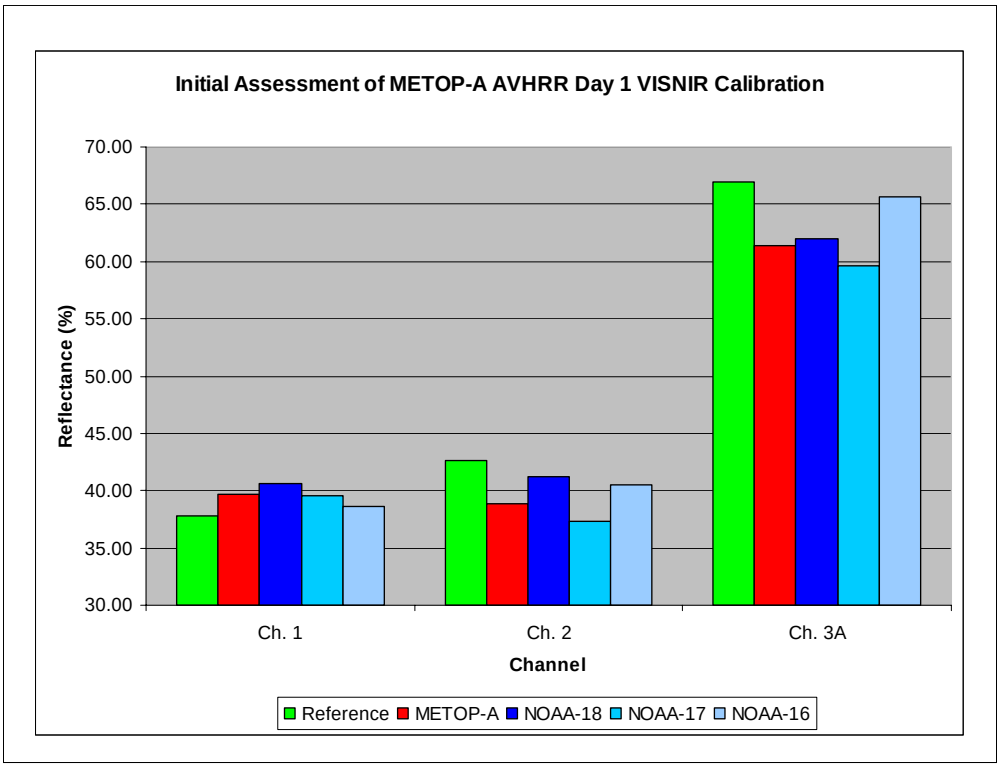

Dr Xiangqian (Fred) Wu's initial findings for the Metop-A AVHRR A305 Visible channel vicarious calibration; using the Libyan Desert target. Green color is the "standard", red color is the Metop-A results. He recommends multiplying prelaunch count-to-reflectance coefficients by 0.97 (ch. 1), and by 1.11 for chs. 2, and 3A.

SNO's

Simultaneous
Nadir
Overpass

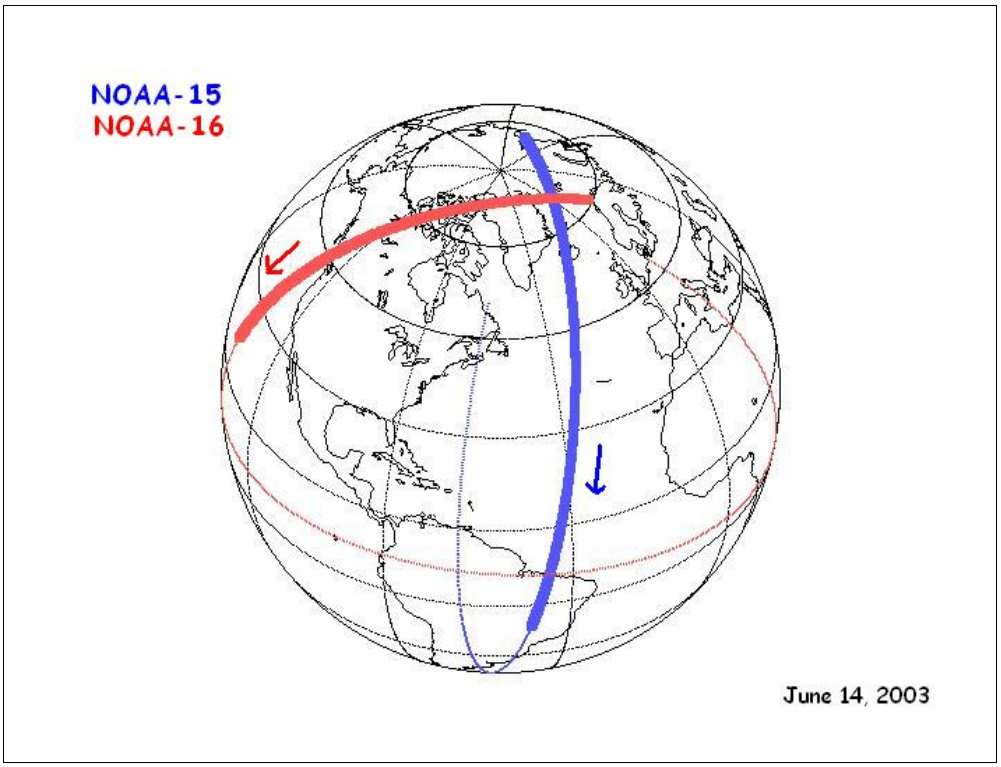

Simultaneous Nadir Overpass. Dr. Cao's excellent idea.

Rocket Science !! All AVHRRs are on polar-orbiting satellites at an altitude of 850 km, which means that every 100 minutes or they will have passed close to both Poles. (The "highest" nadir pixel is over 82N or 82S.) Think of orbits as rings, under which the Earth spins. The 2 rings intersect each other in 2 places, near each Pole. But the close intersection of the nadir pixels from each satellite on the ground may be 10 minutes off. However, satellites closer to the Earth orbit quicker, basically to couteract the stronger gravity pull. Morning satellites (N-15) are closer to the Earth (~ 830 km away) so their orbital time is about 101 minutes; afternoon satellites are higher (N-16 is about 870 km), so the orbital time is ~ 102 minutes. If the morning (quicker) satellite is 10 minutes late one orbit, it will be only 9 minutes late the next orbit, 8 minutes the orbit after that, … until finally the intersection times will almost match within seconds or part of a minute. This is great for Inter-Calibration, both AVHRRs looking at the same targets at the same time !!

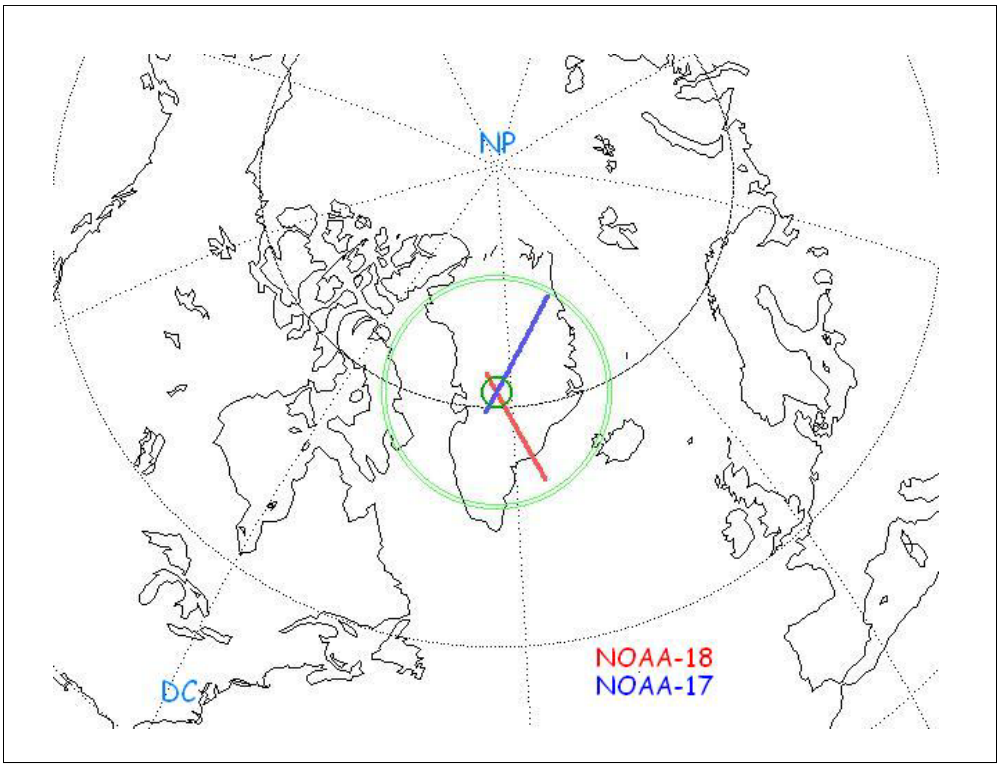

SNO example. An area in central Greenland located around ~ (44W,71N); date is 6/19/2005. The two satellites looked at the same nadir pixel (and surrounding area) approximately 52 seconds apart. I just grabbed this example BUT it turned out to be probably the best example I have. I believe central Greenland is extremely homogeneous, so any navigation problems are minimized.

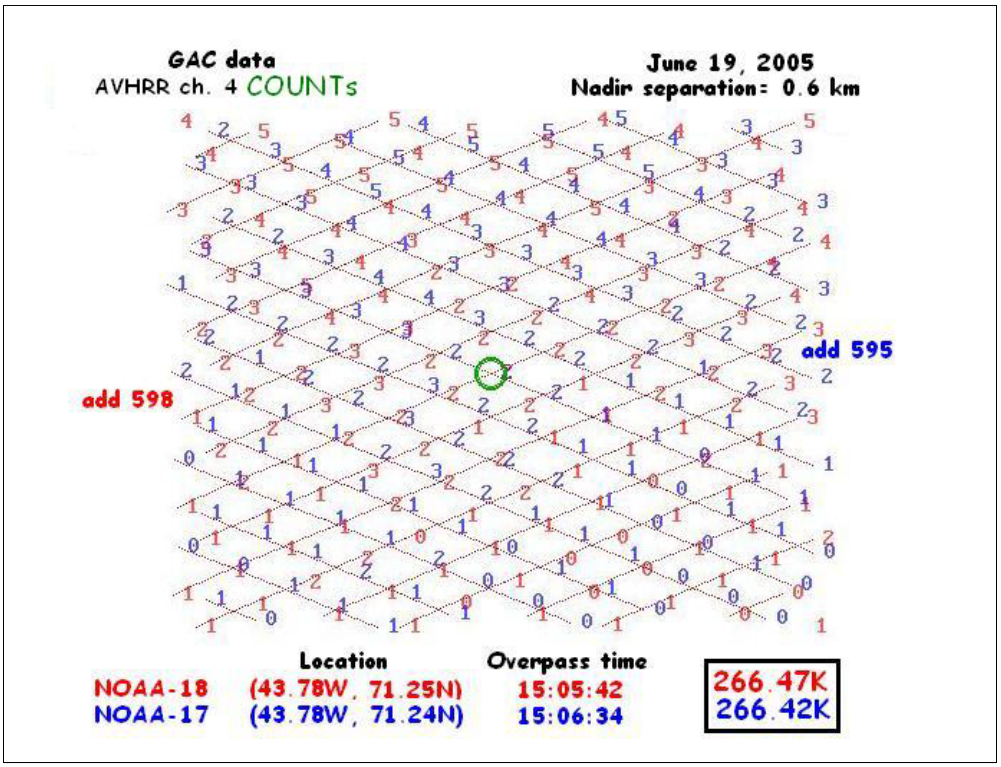

SNO example using AVHRR GAC (3km x 5km) thermal channel 4 data. {N-18 is in red, N-17 is in blue} This 156-pixel GAC array is a little smaller than Rhode Island, USA.

These are AVHRR thermal channel 4 counts, the raw output from the radiometer. To plot small numbers, I subtracted 595 counts from the N-17 output and 598 counts from the N-18. The gradient match is excellent, with both AVHRR “counts” being about 5 near the top of the image and near 0 near the bottom. 1 count = ~ 0.12K.

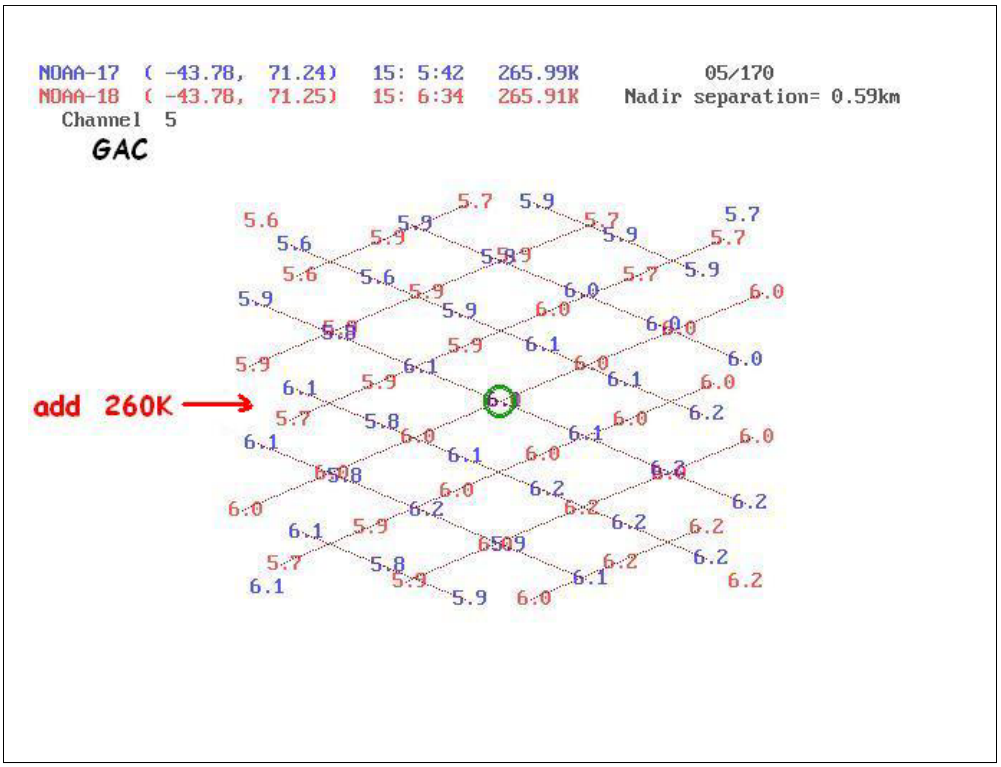

Same general area (a little smaller) but a different channel. These are AVHRR thermal channel 5 temperatures. Again the gradients match well and the areal averages are within 0.1K of each other.

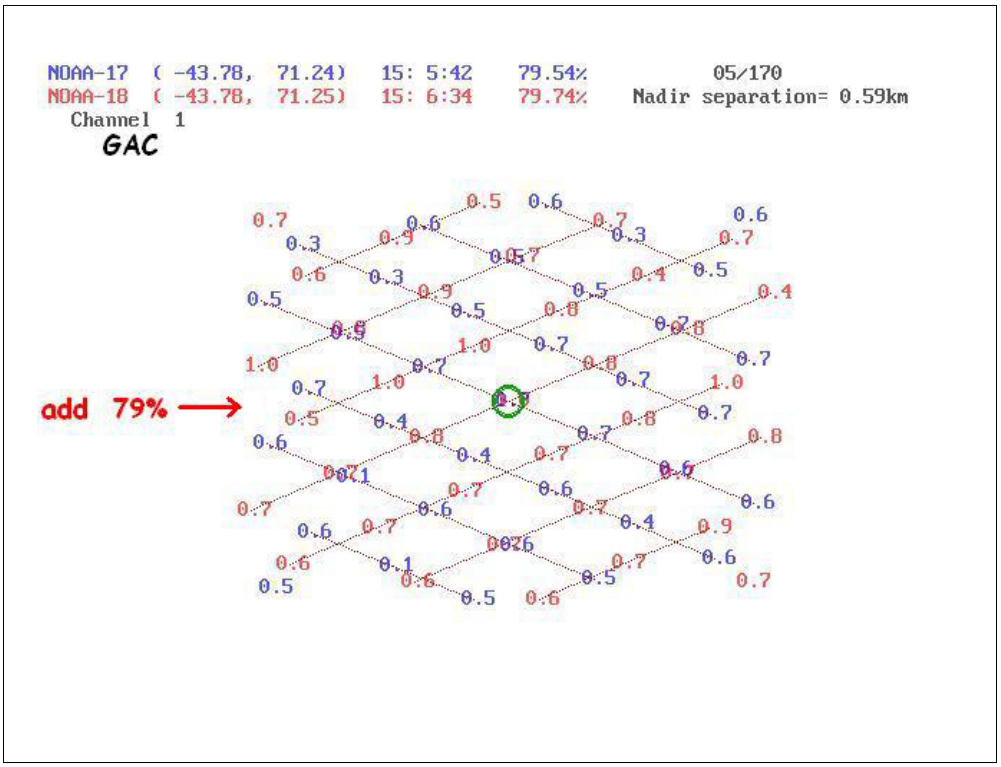

VISIBLE channel 1 reflectances from the same Greenland SNO. Both satellites were calibrated using the vicarious count-to-reflectance coefficients provided by Fred Wu. For both reflectances to match so well (area-averages within 0.5%) is very surprising; perhaps it's a fluke.

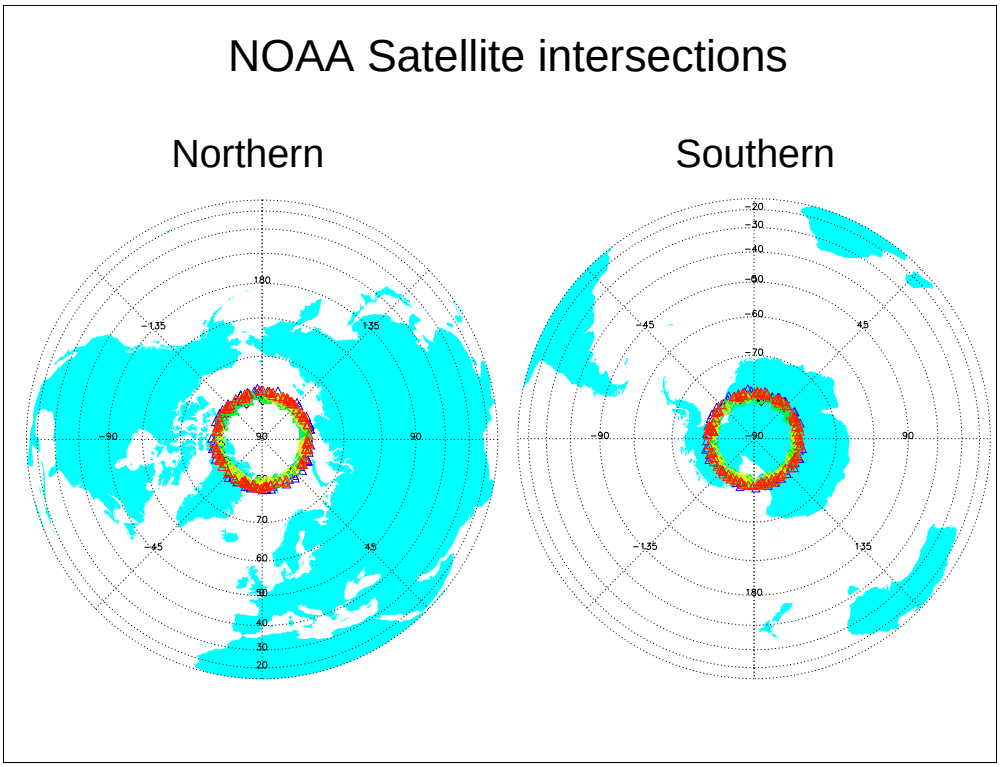

Location of SNOs near the North and South Poles. They usually occur around 80N or 80S. {less frequently around 70N or 70S}

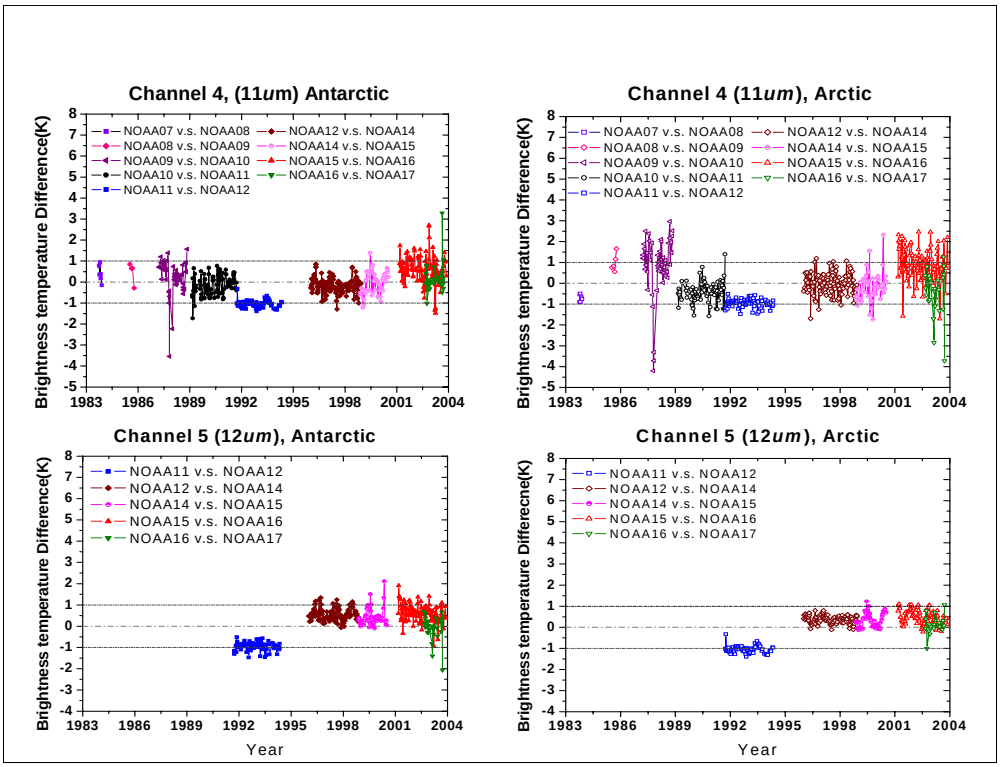

SNOS used to inter-calibrate AVHRR thermal channels 4 and 5 for AVHRRs on NOAA-07 through NOAA-17. The biases are relatively consistent. Figure from PuBu CiRen.

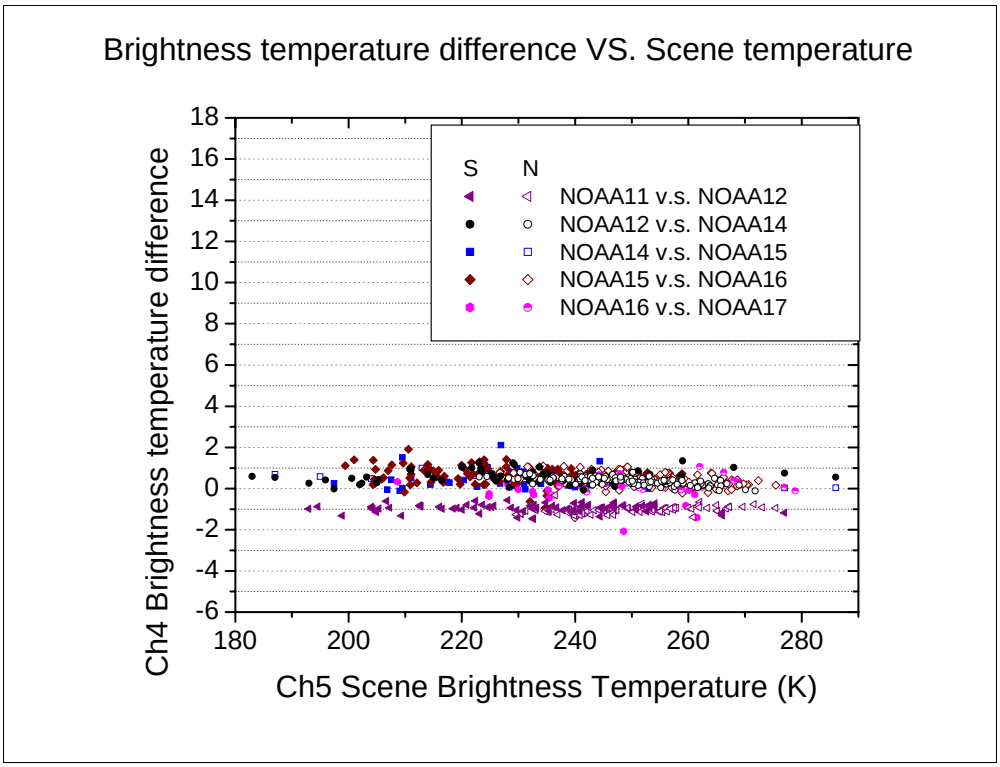

Even though SNOs between polar-orbiters occur only near the Poles, they occur during both winter and summer so the range of temperature is decent. There is about a 90K range, from 190K to 280K. This range does not cover much of the SST range or hotter land surfaces. The data show that the biases are independent of scene temperature.

Example of SNO's for one month of PATMOS-x data (July 1992)

For July 1992, NOAA-11 and NOAA-12 gave 78 grid-cells that met SNO criteria. Note dark counts are removed so line should pass through origin.

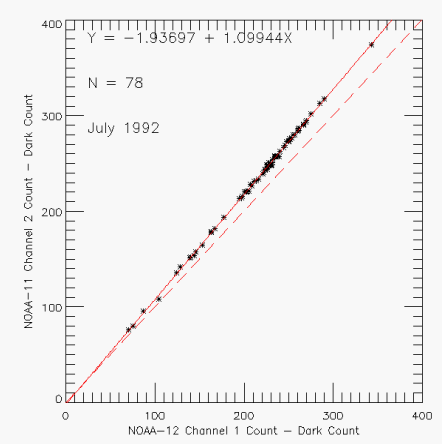

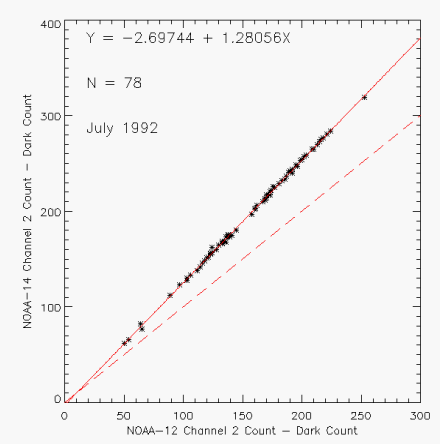

This data provides a constraint on the ratio of NOAA-11 to NOAA-12 calibration slopes. Does not provide any information on absolute calibration by itself.

Use of SNOs to inter-calibrate the visible channels for all NOAA AVHRRS. Data from Andy Heidinger. This shows the strong linear relation between channel 2 counts from the NOAA-11 and NOAA-12 AVHRRs for the month of July, 1992. The relation changes steadily from month to month, showing the **relative** degradation between the channel 2 sensors on these two AVHRRs. Systematic application of this process between the morning and afternoon pairs of AVHRRs allows the entire 14-AVHR time series to be **relatively** inter-calibrated.

Comparison of Ch 1 Equations for NOAA-7,9,11,14,16

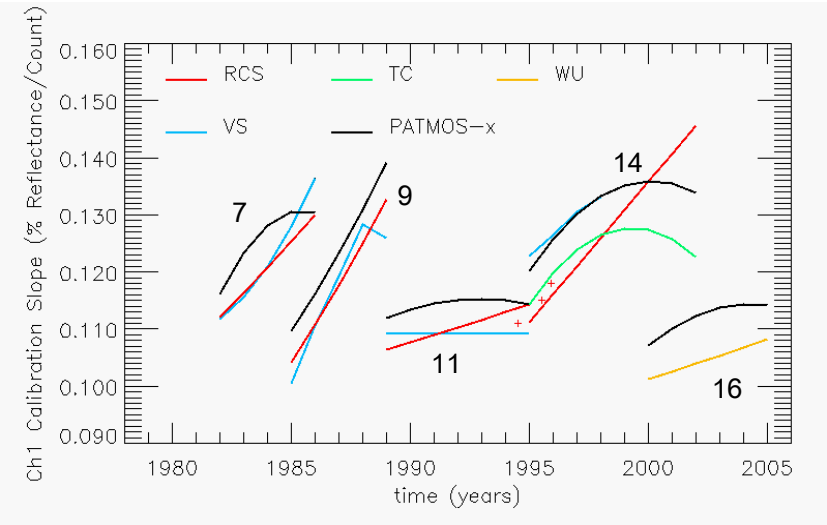

RCS = Rao, Chen and Sullivan
TC = Tahnk and Coakley
VS = Vermote and El Saleous
WU = Fred Wu (Operational NOAA)

The results of using the SNO events to model AVHRR visible channel 1 count-to reflectance conversion coefficients as a function to time, for the afternoon satellites. In prelaunch the coefficient is typically around 0.10% / count. Higher values indicate that the channel response has dimmed in time, so a larger multiplier is needed to counteract this. The relative response corrections agree well with other researchers results.

Comparison of Ch 2 Equations for NOAA-10,12,15 and 17

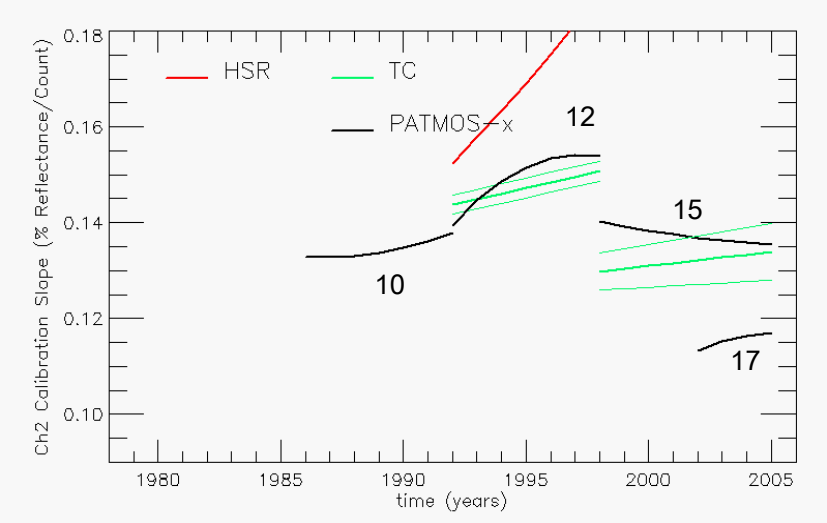

HSR = Heidinger, Sullivan and Rao
WU = Fred Wu (Operational NOAA)

TC = Tahnk and Coakley

The results of using the SNO events to model AVHRR visible channel 2 count-to reflectance conversion coefficients as a function to time, for the **morning** satellites. Finding the relative response decay for AVHRRs on morning satellites is usually more difficult, so few other groups have calculated it.

.

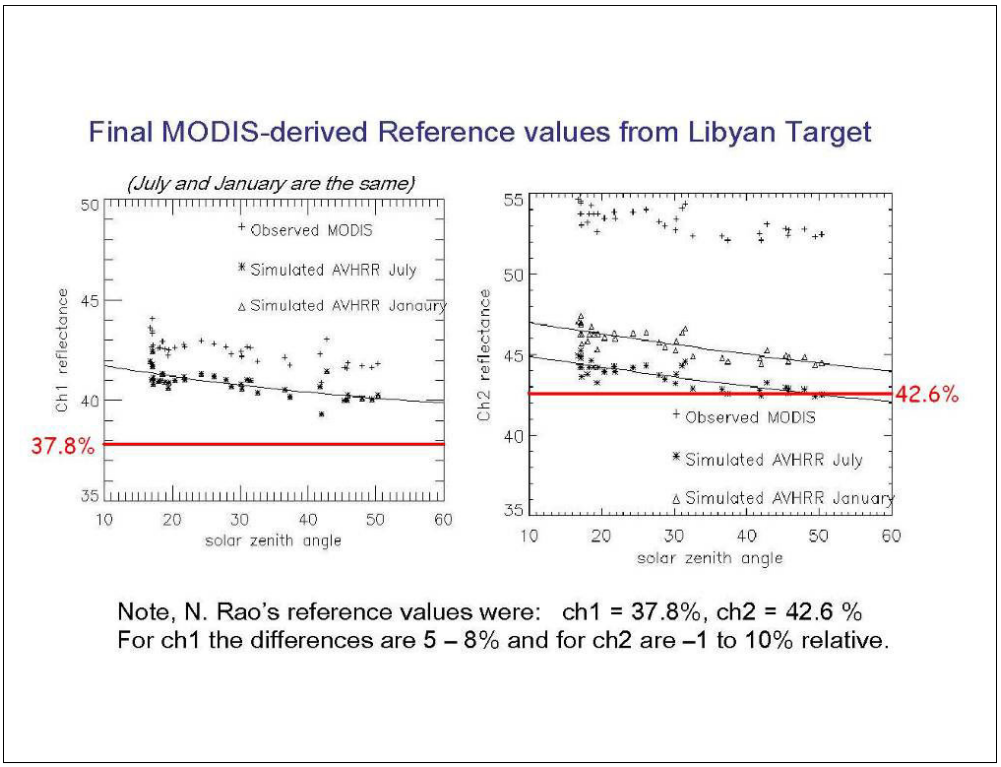

Absolute Calibration for the Libyan Desert. The MODIS instrument has onboard calibration, which we assume is correct. For the 0.65 micron MODIS visible channel, the MODIS measures reflectance values in the 42-43% range. The MODIS visible channel has a somewhat different Spectral Response Function (SRF) than the AVHRR visible channel. These two channels respond differently to atmosphere water vapor and reflected energy from the surface. These effects are modeled and MODIS measurements are used to predict what the AVHRR channel 1 should measure for the Libyan Desert target. The result is in the 40-41% range. However, based on aircraft measurements taken 20 years ago, at NESDIS we have always used 38% as the reference AVHRR ch.1 values for the Libyan Desert target. This discrepancy is just large enough to be suspicious; we are investigating why it occurs.

SNO's / MSU calibration

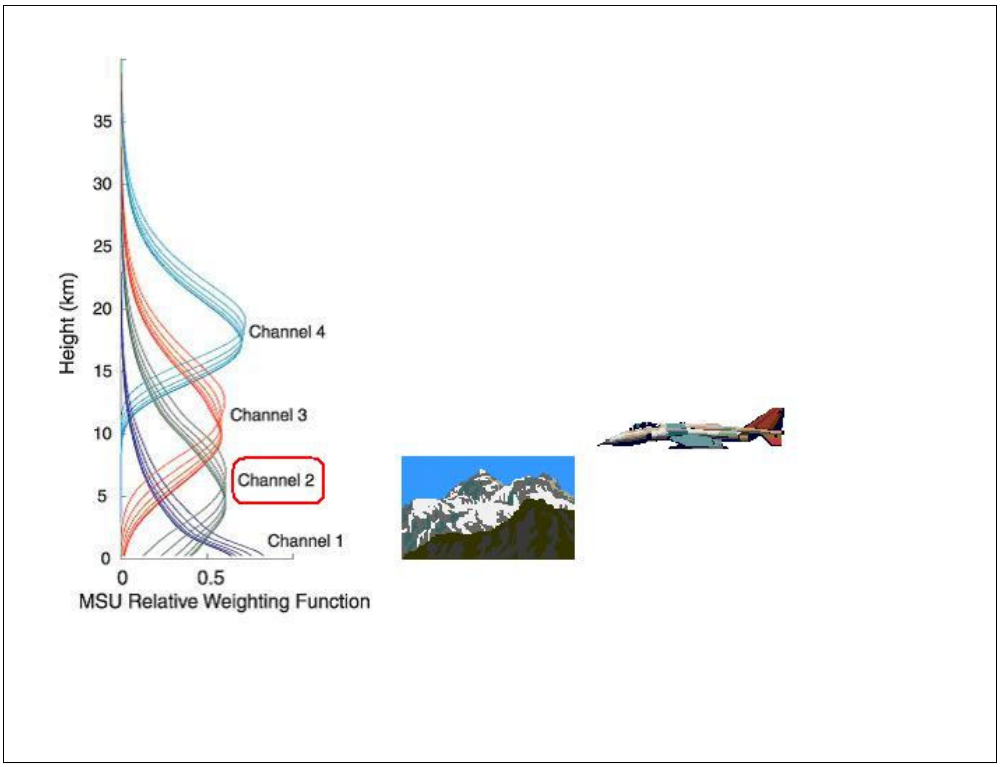

MSU (Microwave Sounding Unit) channel 2 is an atmospheric sounding channel that peaks around 7-8 km. This provides mid-troposphere layer temperature. MSU channel 2 temperatures have some nice features, such as not being affected much by clouds and the fact that MSU Spectral Response Functions are very stable among the instruments so that the same atmospheric layer is always sampled.

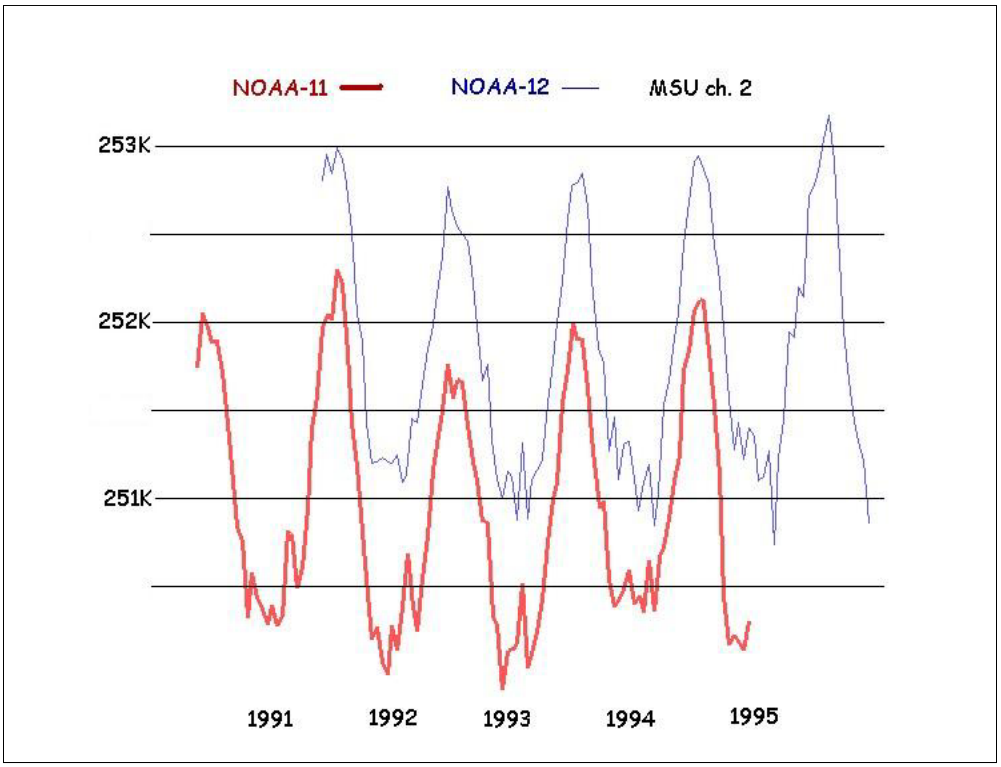

MSU channel 2 temperatures also have some not-so-nice features, such as the fact that when globally-averaged temperature time series are plotted, an obvious bias is apparent. This shows the NOAA-11 and NOAA-12 time series; there is a bias of about 0.8K between them. This bias must be accounted for in any temperature trend work.

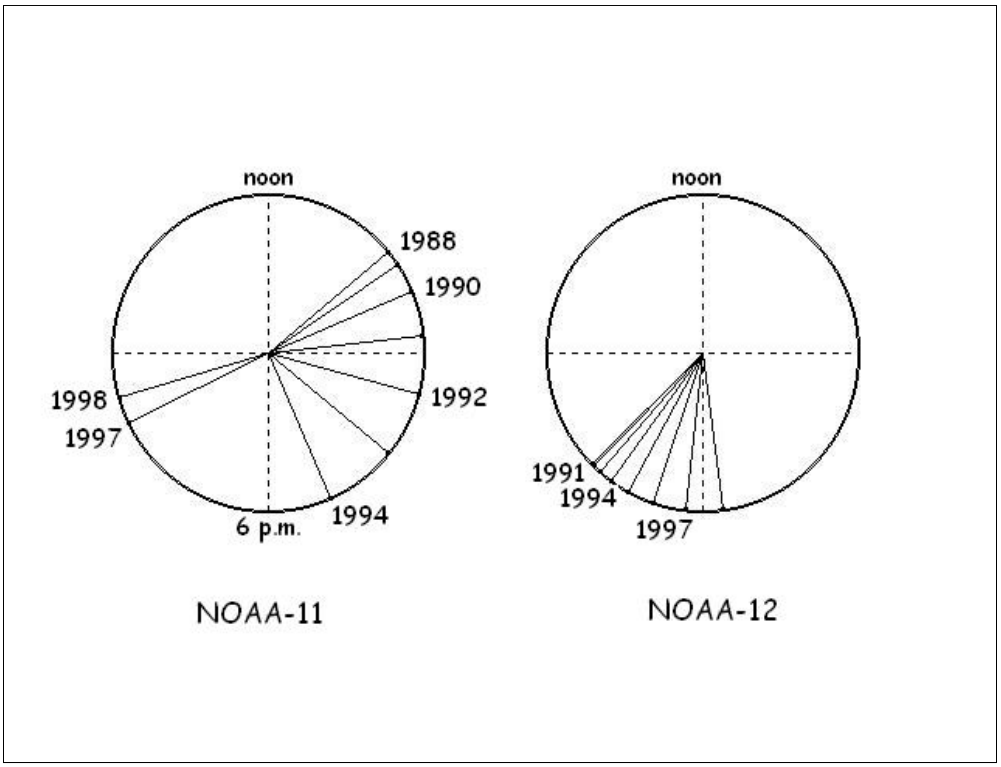

Orbit drift. Before NOAA-15, the orbits of the NOAA polar-orbiting satellites changed noticeably during the satellite lifetimes. The afternoon satellites orbits changed much more than the morning satellites. Measuring a N-11 temperature at 2:00 in 1988 is much different than measuring a N-11 temperature at 6:00 in the afternoon in 1995. This effect also has to be accounted for in determining temperature trends.

Comparison Between Pre-launch and SNO calibrations

Tb time series after pre-launch operational calibration

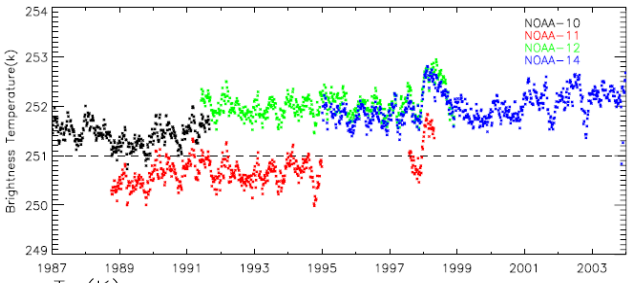

Tb time series after post-launch SNO calibration

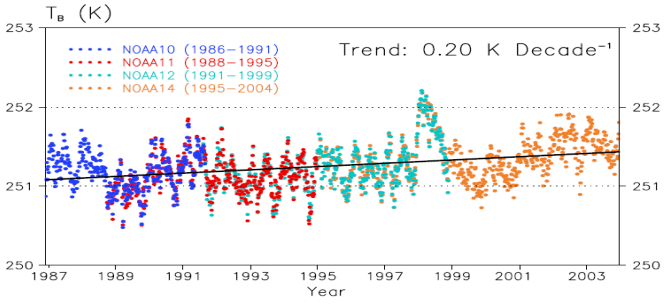

Using SNO events to re-calibrate MSU data results in a different dataset than the NESDIS operational 1b dataset. What is the consequence for the MSU ch. 2 temperature time trend? The 2 figures above show the 5-day global ocean time series, using the NOAA-10, -11, -12, and -14 MSUs. Large inter-instrument biases have nearly disappeared from the SNO time series. The trend associated with the SNO-calibrated dataset is about 0.20 K / decade. This is an ongoing and still somewhat controversial result. Data from Cheng-Zhi Zou.

Navigation

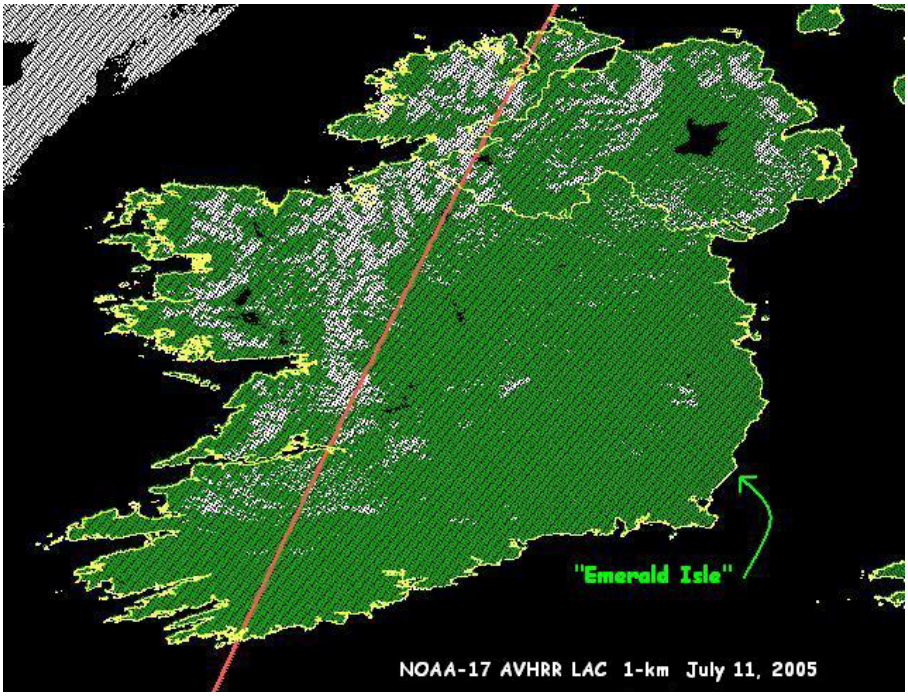

Basic principle for monitoring navigation (geo-location) accuracy. Data from AVHRR visible channels 1 and 2 is used to generate a “veggie” index, the NDVI (Normalized Vegetation difference Index). This index distinguishes very well between land and water. Values of NDVI for land are colored green, values for water are colored black, and plotted on a simple lat/long projection, using the (long,lat) data given in the AVHRR 1b file. The yellow dots are (long,lat) values from the WVS (World Vector Shoreline) geography file. It is stated that these points have an accuracy of 0.5 km, 90% of the time. If the NDVI map matches the yellow border well, then the AVHRR navigation is good. The scale is such that 1 pixel on the screen is 1 AVHRR pixel (1knm x 1km at nadir). For this NOAA-17 scene, the navigation looks to be accurate to within 1 pixel.

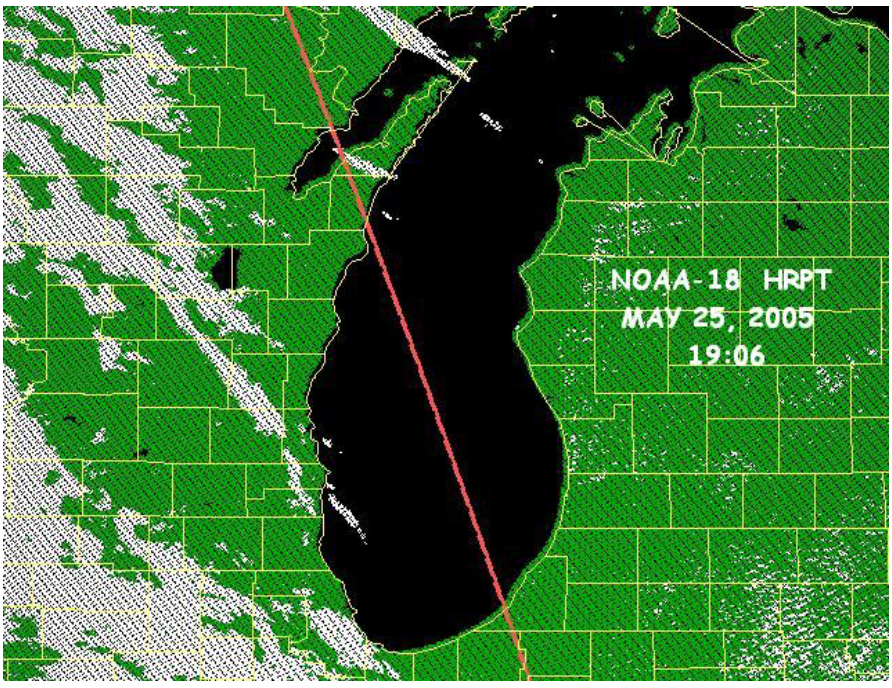

NOAA-18 navigation. For this early N-18 scene, AVHRR 1b navigation looks to be off by 3-4 pixels. {Pixel size is 1km x 1km at nadir.}

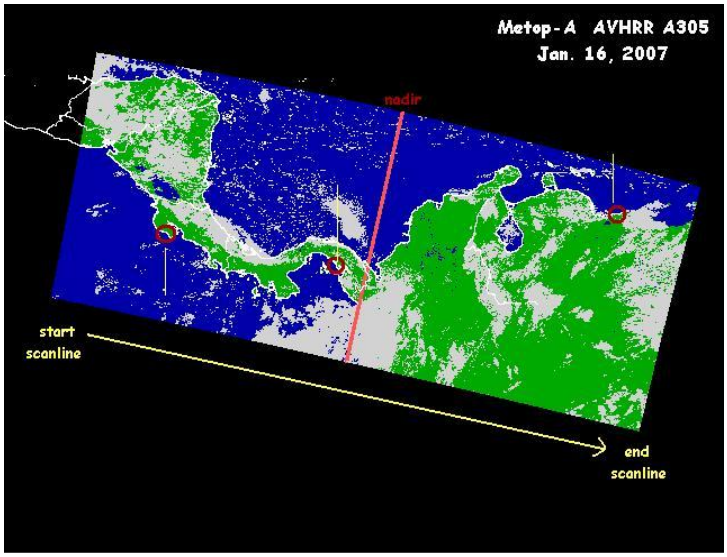

Figure 6. A geo-location test area in Central and South America (Panama Canal). Scanlines start on the left of the image. Areas under the three red circles will be magnified in the next three Figures.

Metop-A AVHRR A305 navigation is a different ballgame. Navigation errors in previous NOAA satellites were often along-track (pitch) errors, sometimes caused by timing errors. {1 second error = 7 km error.} The Metop-A satellite is purposely moved in the yaw direction as it goes through each orbit, to help the ASCAT microwave instrument measure ocean surface winds. The movement is largest at the Equator and approaches zero near the Poles. If this is not accounted for, errors larger than 20 km occur. Even after corrected for the yaw movement, we find that NESDIS Operations Metop-A AVHRR 1b navigation still has smaller but repeatable errors. The pattern is: a 1 pixel error at the start of each scanline, 1-2 pixel error near nadir, and 3-4 pixels error near the end of a scanline. This is for scanlines near the Equator; I have not checked near the Poles yet.

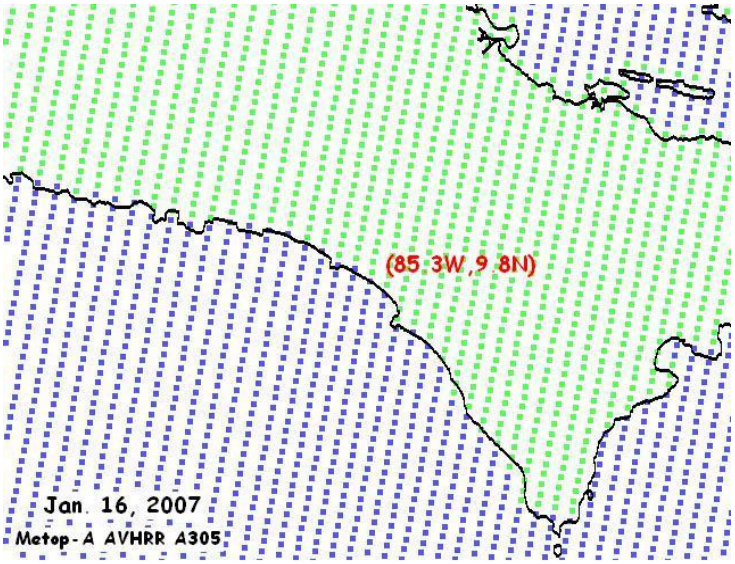

Figure 6a. Near the start of each scanline, the land/sea separation indicated by the NDVI (green vs. blue pixels) matches the WVS shoreline boundary (black line). Geo-location accuracy is very good.

Start of scanlines. The land/sea boundary (green/blue) indicated by the NDVI index matches the WVS shoreline (black) very well.

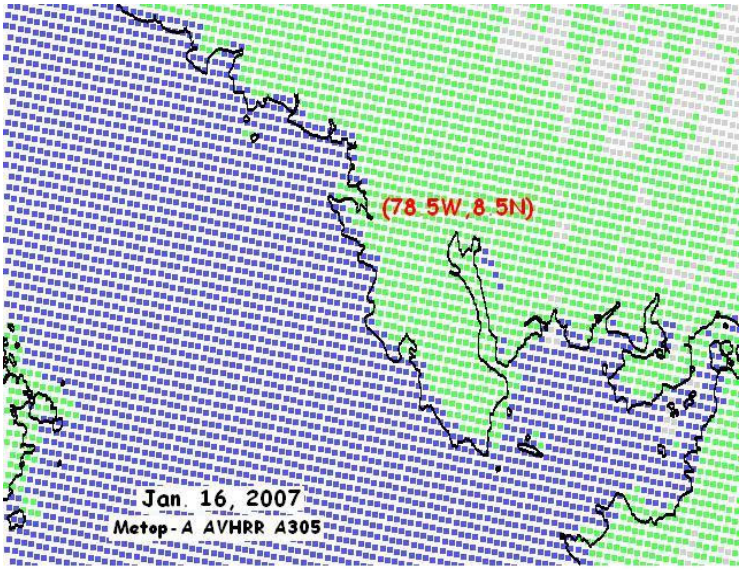

Figure 6b. Near the middle of each scanline, the land/sea separation indicted by the NDVI (green vs. blue pixels) is 1-2 AVHRR pixels off from the WVS shoreline boundary (black line).

Near nadir. The match is slightly off, maybe 1-2 pixels.

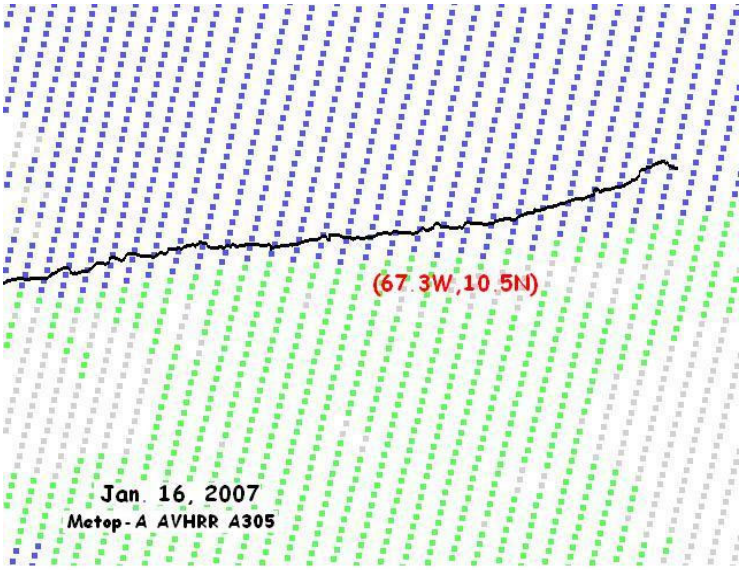

Figure 6c. Near the end of each scanline, the land/sea separation indicated by the NDVI (green vs. blue pixels) is 3-5 pixels off from the WVS shoreline boundary (black line).

End of scanlines. Differences of 2-4 pixels between AVHRR 1b navigation and the WVS boundary are apparent.

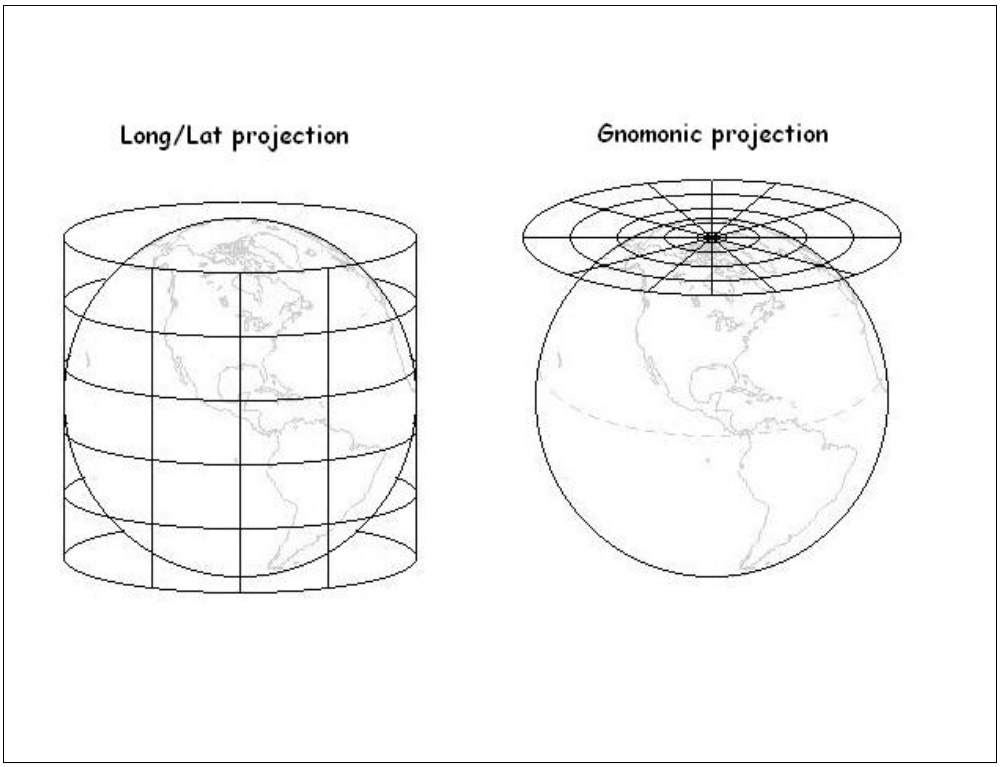

Further navigation note. Each AVHRR 1b LAC scanline has count values for 2,048 pixels. However, to save space, (long,lat) locations are only given for 51 anchor pixels {every 40th pixel}. Locations for the other 97% of the pixels must be interpolated using the anchor pixel locations. Usually, latitudes and longitude values are interpolated separately, using linear or quadratic interpolation. This is a good strategy near the Equator (and quite far from it also). However, near the Poles, greater than 85N or 85S, this is a bad idea. Projections of the Earth are generally useful near regions where they touch the Earth. The left image shows that the Long/Lat projection is not useful near the Poles. The right image shows the Gnomonic projection, which is very much like the Polar Stereographic; it is useful near the Poles. The bottom line is: near the Poles, convert (long.lat)'s to Gnomonic coordinates, do the interpolation in these coordinates, then re-convert the interpolated locations back to (long,lat)'s.

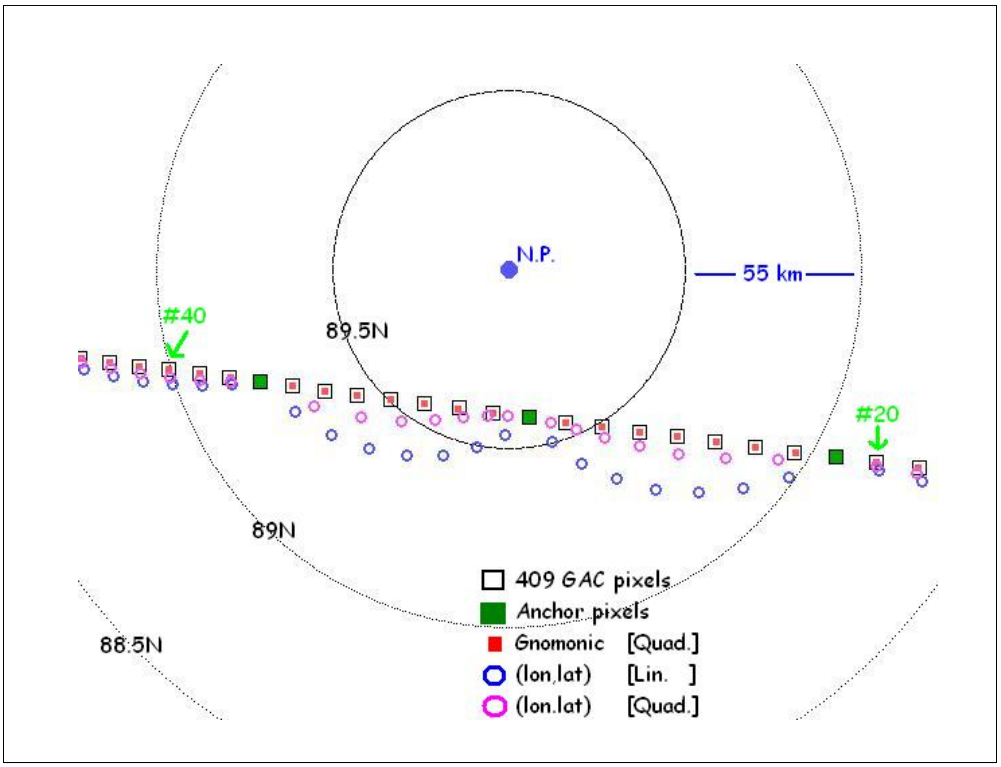

Open black squares are AVHRR GAC (3km x 5km pixel size) locations, computed by Alek Jelenak using the SGP4 orbital model. In the 1b dataset, only locations for the solid green squares are given, the anchor pixels. The blue circles show the results of linear interpolation in longitude and latitude separately; errors of up to 17 km. The purple circles show the results of quadratic interpolation in longitude and latitude separately; errors still up to 10-15 km. The solid red squares are the results of using Gnomonic interpolation; they fit nicely within the black squares, errors ~ **0.3 km.**

CREDITS

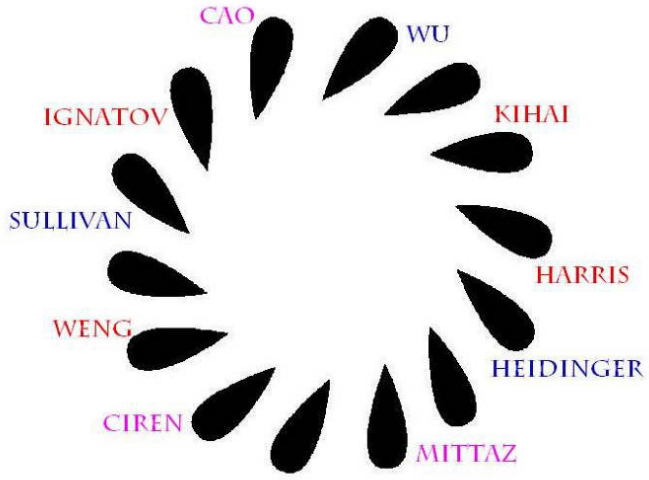
CAO
WU
IGNATOV
KIHAI
SULLIVAN
HARRIS
WENG
HEIDINGER
CIREN
MITTAZ

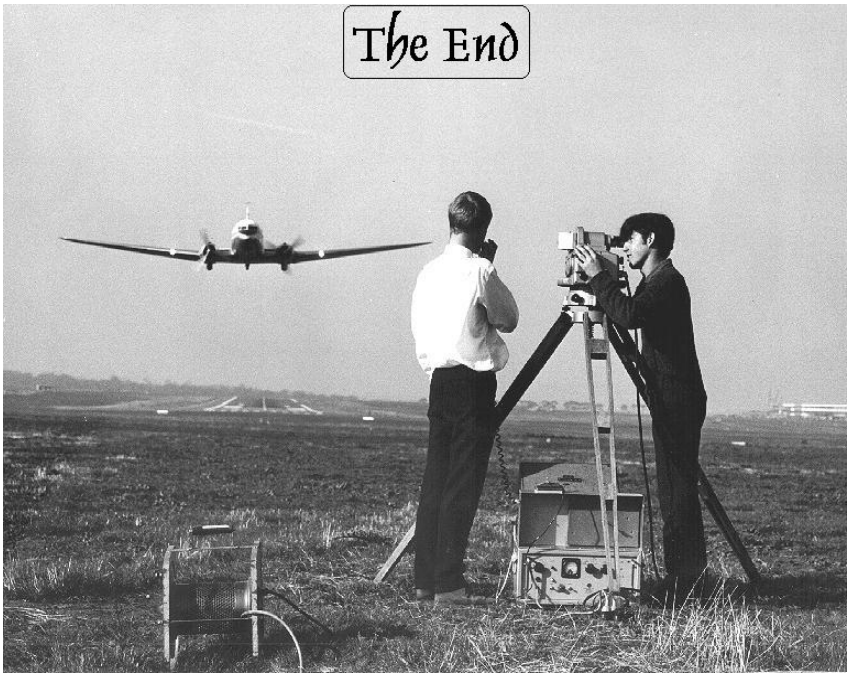
The End

BACKUP SLIDES

The radiance R_{BB} from the internal blackbody at temperature T_{BB} is the weighted mean of the Planck function over the spectral response of the channel.

From NOAA-15 on, ITT measures the spectral response function for each channel is measured in approximately 200 wavelength intervals. Using these, NESDIS generates a look-up table where, for all temperatures between 180K and 340K in steps of 0.1K, the table specifies the AVHRR radiance.

The following two-step equation accurately reproduces Energy Table equivalent blackbody temperatures to (usually) within ± 0.005K in the 180 to 340K range;

$$T_{BB}^{*} = A + B \cdot T_{BB} \qquad \text{(“effective” temperature)}$$

$$R_{BB} = c1 \cdot \nu_C^{3} \; / \; [\exp(c2 \cdot \nu_C / T_{BB}^{*}) - 1]$$

where c1 and c2 are the first and second radiation constants.

R_{BB} can be written as:

$$R_{BB} = R_0 \; / \; [\exp(T_0 / T_{BB}^{*}) - 1] \qquad \mathbf{R_0 \equiv c1 \cdot \nu_C^{3}}, \quad \mathbf{T_0 \equiv c2 \cdot \nu_C} \; .$$

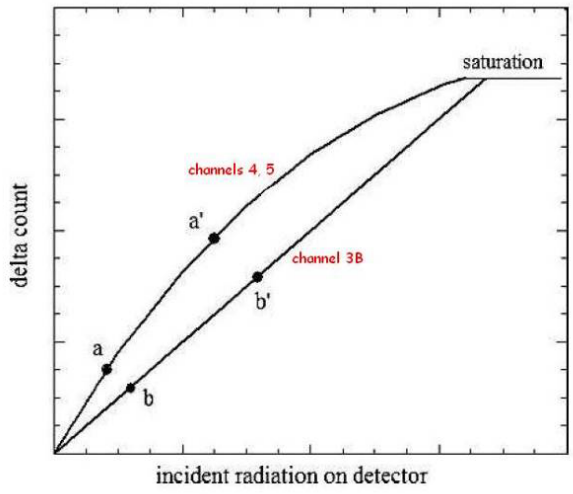

The effect of nonlinearity and self-emission. At blackbody temperature Ta, the instrument gain is at point a. Changing the temperature to Ta' causes more incident radiation on the detector, and the AVHRR gain shifts to point a'. This is for channels 4 and 5. Channel 3B is more linear; points b and b' have (nearly) the same gain.

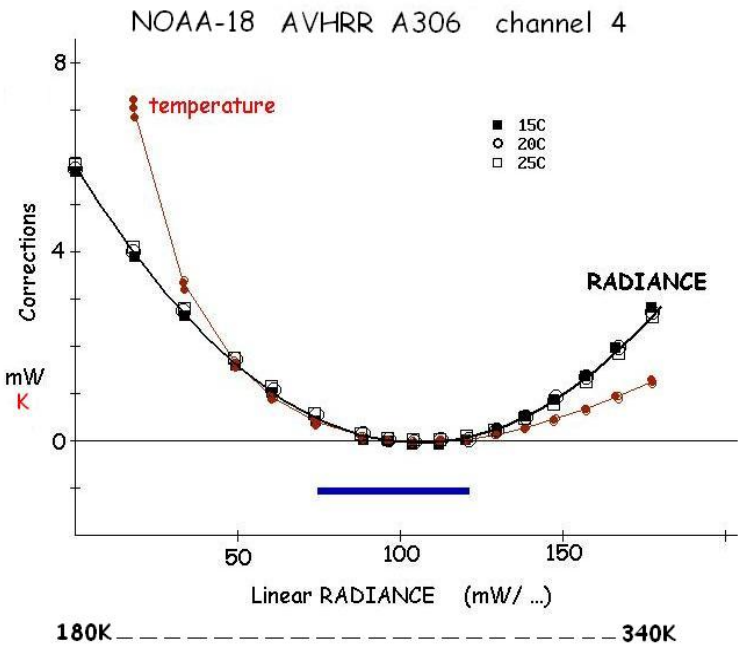
NOAA-18 AVHRR A306 channel 4
temperature
15C
20C
25C
RADIANCE
Corrections
mW
K
8
4
0
50
100
150
Linear RADIANCE (mW/ ...)
180K
340K

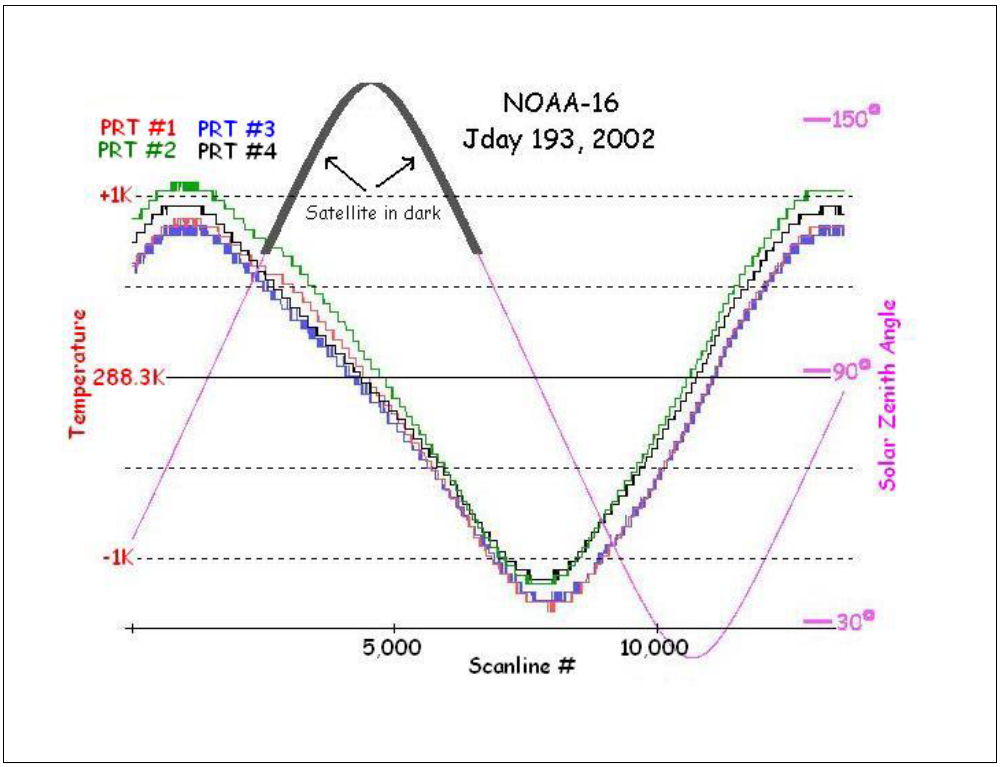
NOAA-16
Jday 193, 2002
PRT #1
PRT #2
PRT #3
PRT #4
Satellite in dark
+1K
288.3K
-1K
Temperature
150°
90°
30°
Solar Zenith Angle
5,000
10,000
Scanline #

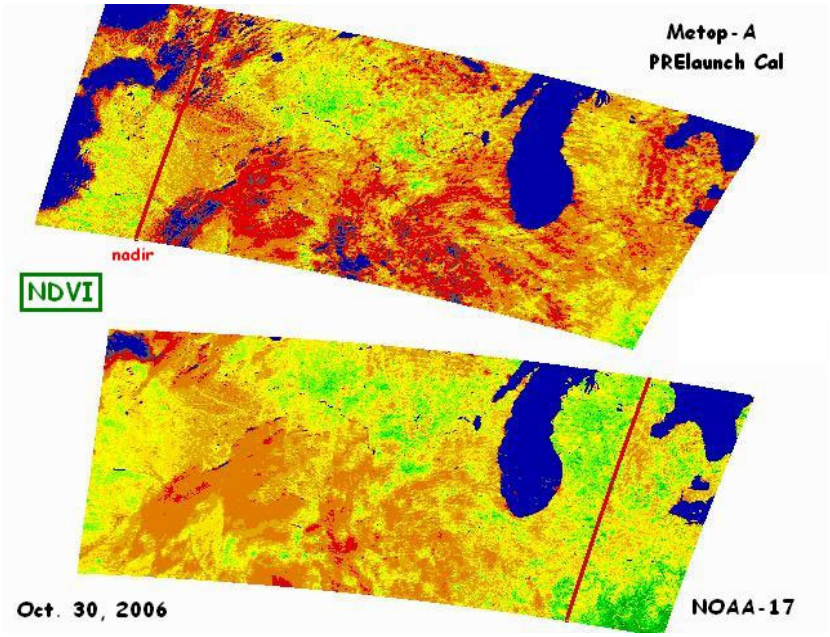

This image compares NDVI (Normalized Difference Vegetation Index) from the Metop-A VAHRR A305, using PRELAUNCH calibration coefficients for channels 1 and 2, to NDVI values from the NOAA-17 AVHRR.

GREEN = high YELLOW = medium ORANGE/RED = low { NDVI }

Both Metop-A and NOAA-17 are morning satellites. The match of the two NDVI images is OK but not great. The match is also complicated by the fact that one AVHRR receives backscattered radiation (check the red nadir lines) and the other gets forward scattered radiation. This is known to produce different NDVI values from the same scene.

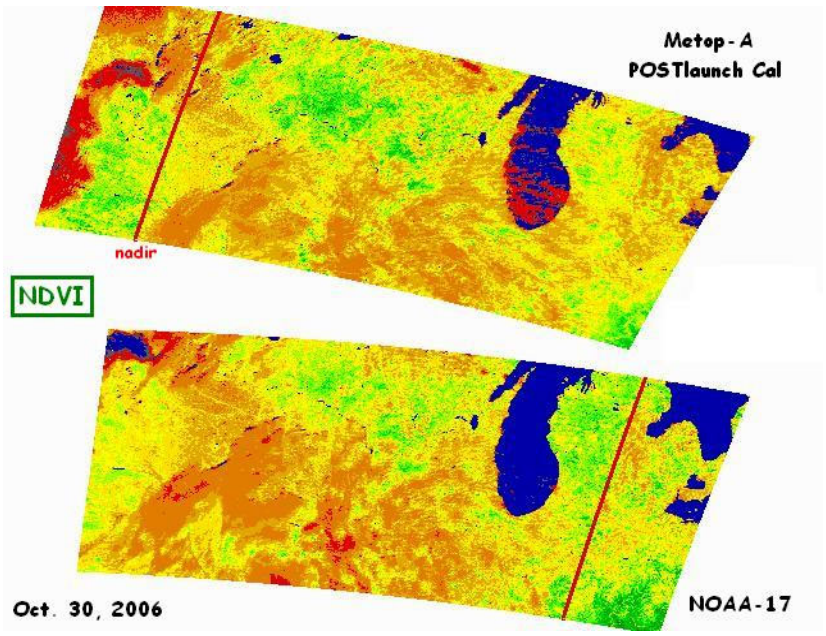

This image compares NDVI (Normalized Difference Vegetation Index) from the Metop-A VAHRR A305, using POSTLAUNCH calibration coefficients for channels 1 and 2 provided by Dr. Wu on 1/8/07, to NDVI values from the NOAA-17 AVHRR.

GREEN = high YELLOW = medium ORANGE/RED = low { NDVI }

Both Metop-A and NOAA-17 are morning satellites. The match of the two NDVI images is an improvement over the comparison using PRElaunch Metop-A coefficients but is still not exact.

Example of one July's SNO's for ch1 and ch2 of TERRA and NOAA-16

(note y-axis should be ch1 nor ch2 on left-hand plot)

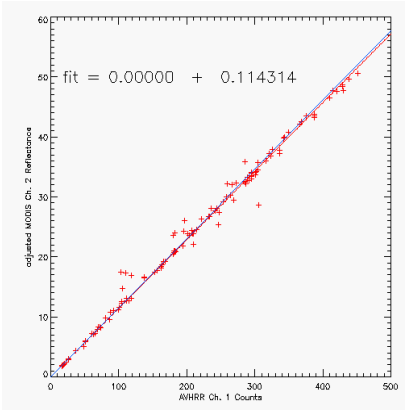

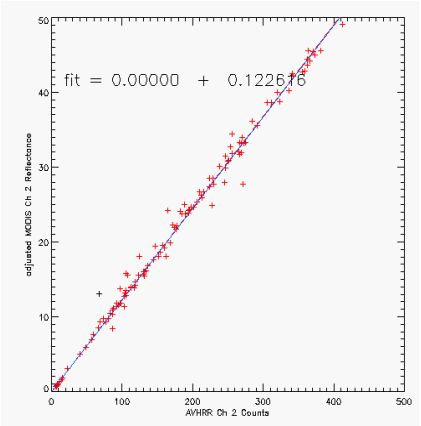

Note, MODIS reflectances are adjusted for mean sun-earth distance *(because this is the quantity used in the standard AVHRR reflectance calibration)*

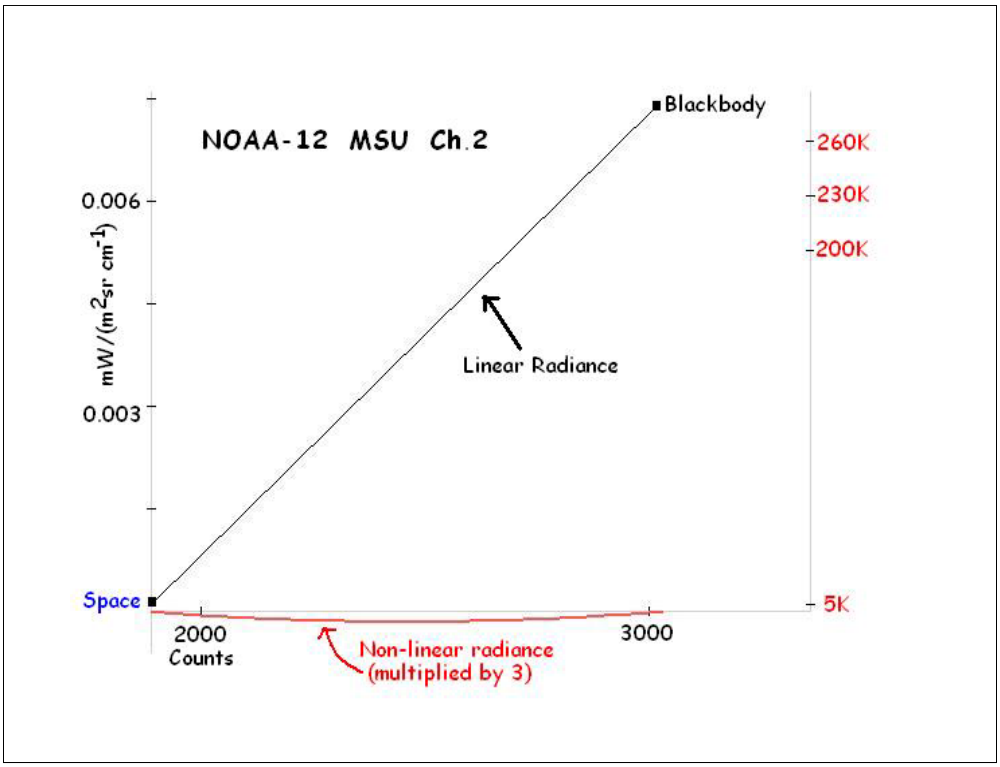
NOAA-12 MSU Ch.2
Blackbody
260K
230K
200K
0.006
0.003
mW/(m2sr cm-1)
Linear Radiance
Space
5K
2000
Counts
3000
Non-linear radiance
(multiplied by 3)

Comparison Between Pre-launch and SNO calibrations

Inter-satellite difference after pre-launch operational calibration

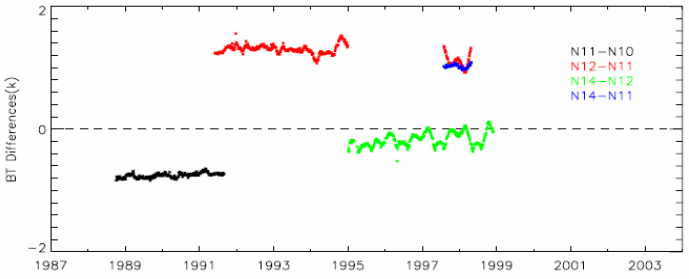

Inter-satellite differences after post-launch SNO calibration

std=0.03K

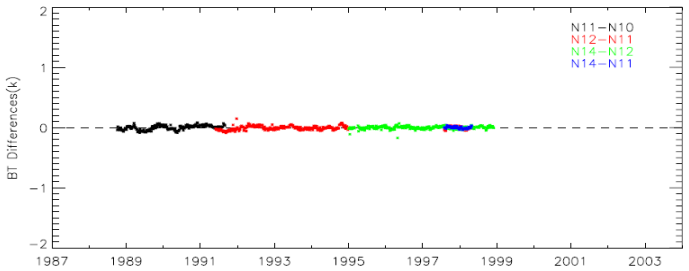

These plot show details of the intersatellite differences between the NESDIS operational calibration and the SNO calibration. The upper plot is the intersatellite differences. We see there are large biases between intersatellite differences an the differences are a function of the warm target temperature. After the SNO calibration, the biases can be reduced to near zero and warm target temperature contamination is removed as well.

Pixel #	LINEAR Gnom.	(lon,lat)	QUADRATIC Gnom.	(lon,lat)
8	3.6	4.1	0.8	2.4
9	3.7	4.3	0.8	2.3
10	3.5	4.1	0.8	2.0
11	2.7	3.2	0.5	1.4
12	1.6	1.9	0.4	0.8
14	1.3	2.6	0.1	0.7
15	2.0	4.3	0.2	1.3
16	2.5	5.3	0.2	1.8
17	2.4	5.5	0.5	2.1
18	2.4	5.2	0.3	2.0
19	1.9	4.1	0.3	1.7
20	1.2	2.4	0.1	1.1
22	0.8	8.0	0.1	6.0
23	1.2	13.5	0.1	10.1
24	1.7	16.8	0.3	12.1
25	1.7	17.6	0.2	12.3
26	1.6	16.3	0.1	11.0
27	1.2	12.8	0.1	8.3
28	0.7	7.3	0.0	4.5
30	0.6	7.6	0.1	4.7
31	1.0	13.5	0.2	9.3
32	1.3	17.0	0.2	13.1
33	1.4	18.3	0.2	15.6
34	1.3	17.3	0.2	16.1
35	1.0	13.9	0.1	14.1
36	0.5	8.2	0.2	8.9

(km)

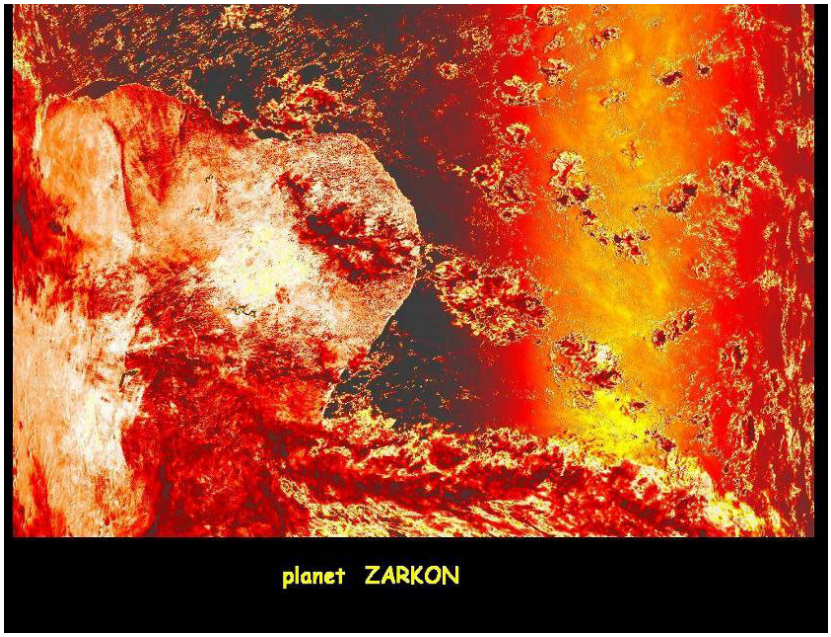
planet ZARKON